Sustainable Food Technology

Accepted Manuscript

This article can be cited before page numbers have been issued, to do this please use: S. Mariño-Cortegoso, R. Tolve, A. Rodríguez-Bernaldo de Quirós, R. Sendón, F. Favati and L. BARBOSA-PEREIRA, *Sustainable Food Technol.*, 2026, DOI: 10.1039/D6FB00090H.

ROYAL SOCIETY OF CHEMISTRY

View Article Online
DOI: 10.1039/D6FB00090H

USC UNIVERSIDADE DE SANTIAGO DE COMPOSTELA

FoodChemPack
RESEARCH, DEVELOPMENT AND CHEMICAL SAFETY ASSESSMENT ON FOOD AND FOOD CONTACT MATERIALS

Department of Analytical Chemistry, Nutrition and Food Science
FACULTY OF PHARMACY

Letricia Barbosa Pereira, PhD
Associate Professor
letricia.barbosa.pereira@usc.es

Sustainability Spotlight Statement

This study contributes to the United Nations Sustainable Development Goals, particularly SDG 12 (Responsible Consumption and Production), by valorizing lime by-products into a high-value functional ingredient within a circular economy framework, reducing food waste and improving resource efficiency.

Additionally, it aligns with SDG 9 (Industry, Innovation and Infrastructure) through the application of innovative food engineering technologies such as ultrasound-assisted extraction and nano/mini spray-drying for efficient recovery and stabilization of bioactive compounds.

The development of antioxidant-rich, functional food ingredients with enhanced bioaccessibility also supports SDG 3 (Good Health and Well-being), promoting improved nutritional quality and potential health benefits through diet.

Furthermore, by reducing losses of bioactive compounds during processing and enhancing their stability, this work indirectly contributes to SDG 2 (Zero Hunger), supporting more efficient food systems and improved nutrient availability.

Overall, this research demonstrates how sustainable innovation in food processing can integrate waste valorization, technological advancement, and nutritional improvement, contributing to more resilient and sustainable food systems aligned with global sustainability goals.

Sincerely,

Letricia Barbosa-Pereira

View Article Online
DOI: 10.1039/D6FB00090H

ARTICLE

Encapsulation of Lime Extract from By-Products in Zein–Pectin Microparticles for Gluten-Free Vegan Pancakes

Received 00th January 20xx,
Accepted 00th January 20xx

DOI: 10.1039/x0xx00000x

Sandra Mariño-Cortegoso*[a,b], Roberta Tolve*[c], Ana Rodríguez-Bernaldo de Quirós[a,b], Raquel Sendón[a,b], Fabio Favati[c], Letricia Barbosa-Pereira*[a,b]

Amid rising demand for healthier and sustainable foods, this study valorised lime by-products as sources of bioactive compounds within a circular economy framework. Lime extract was encapsulated in zein–pectin microparticles using Nano Spray Dryer (NSD) and scaled up with a Mini Spray Dryer (MSD), both yielding comparable results.

The developed particles showed high encapsulation efficiency (>80%), high yield (>90%), strong antioxidant capacity (>6 mg TE/g), and quantifiable phenolics. Encapsulation improved thermal stability: while free extract lost up to 92% of phenolics after 10 minutes at 200 °C, encapsulated particles retained 52%.

These microparticles were added to gluten-free, vegan pancakes, improving nutritional quality and batter consistency. After *in vitro* digestion, encapsulated phenolics showed at least 10% higher bioaccessibility and recovery than the free extract. Even within the pancake matrix, 60% of phenolics remained bioaccessible, with recoveries above 70%. Overall, lime by-products and spray drying effectively produced stable, functional food ingredients.

1. Introduction

Agri-food by-products are generated throughout the food chain, mainly during industrial processing, which represents one of the greatest challenges in terms of the inefficient use of natural resources[1]. Particularly, citrus fruits are among the most popular and widely consumed fruits worldwide. The high production is related to the generation of tonnes of residues during industrial processing; a mixture of peels, seeds, and pomace that represents around 50% of the fruit weight [2].

Many studies have focused on their valorisation through the extraction and use of bioactive compounds, such as phenolic compounds, with demonstrated antioxidant properties related to health benefits, including effects on cardiovascular protection, lipid metabolism, oxidative stress, and inflammation [3,4].These advantageous properties promote the production of ingredients to develop functional foods [5].

Nevertheless, polyphenols are highly sensitive to heat, light, and oxygen, and many phenolics are unstable during digestion or interact with food matrices in ways that reduce bioaccessibility and alter texture [6,7]. To address these limitations, various protective technologies have been explored. Encapsulation is particularly promising, as it enhances the stability and solubility of phenolic compounds, enables controlled release, and masks off flavours [8,9]. It can also improve their bioaccessibility and bioavailability while supporting beneficial gut microbiota through the metabolites of polymeric polyphenols, ultimately increasing their functional performance in food systems [8,10].

Proteins and polysaccharides from industrial by-products show strong potential as encapsulating materials. Zein, the main corn storage protein, is widely studied as a delivery vehicle due to its amphiphilic nature and ability to form core–shell particles that protect phenolics from adverse conditions, like heat and oxygen [11,12]. Because zein is degraded by proteases, it enables bioactive release in the proximal intestine. Its performance can be enhanced by pectin, a citrus-derived polysaccharide resistant to gastric conditions and known for its emulsifying properties, which improves the stability and functionality of zein particles [13]. Pectin also adds dietary fibre, can replace fat, supports structure in baked goods, and allows extended release of bioactives through colonic fermentation while reducing phenolic metabolization [14,15].

Among encapsulation methods, spray drying is widely used to stabilise core–shell structures and protect bioactives by reducing water-related degradation [16,17]. Nano spray-drying has been developed to obtain lower-size particles, with a greater surface area, which increases their solubility and, consequently, the bioaccessibility of newly produced food ingredients with functional properties [18,19].

Despite rising demand for healthier foods, bakery items are often sugar- and fat-rich, a concern especially relevant for individuals with celiac disease dependent on low-nutrient, high-glycaemic indices gluten-free products [20,21]. Additional dietary

[a] FoodChemPack research group, Department of Analytical Chemistry, Nutrition and Food Science, Faculty of Pharmacy, University of Santiago de Compostela, 15782, Santiago de Compostela, Spain
[b] Instituto de Materiales (iMATUS), University of Santiago de Compostela, Santiago de Compostela, Spain
[c] Department of Biotechnology, University of Verona, Strada Le Grazie 15, Verona, 37134, Italy

restrictions, such as lactose or egg intolerance, further limit the availability of choices and nutritious options. In response, vegan alternatives are gaining popularity for their inclusivity and broader consumer appeal.

In this context, functionalization strategies can improve the nutritional quality of processed foods and meet demand for healthier, allergen-friendly products [22]. Lime by-products are particularly suitable, as they are rich in phenolics such as flavanone glycosides and hydroxycinnamic acids [23].

This study explored the valorisation of lime by-products through the development of zein–pectin microparticles encapsulating lime by-product extracts, with innovation focused on three main aspects. First, it was employed both nano- and mini- spray dryers, with a comparative scale-up investigation conducted by producing particles using both technologies, allowing evaluation of how processing scale can influence particle properties. Comprehensive physicochemical characterisation was performed, alongside the determination of antioxidant activity, total phenolic content, and individual phenolic compounds to assess encapsulation efficiency. Second, the resulting microparticles were applied as functional ingredients in a specific food matrix—vegan and gluten-free pancakes—at two fortification levels by partially replacing the flours in the control formulation. Finally, beyond conventional physicochemical and nutritional analyses of the fortified products, an *in vitro* gastrointestinal digestion was employed to assess the bioaccessibility of phenolic compounds, providing novel insights into the effectiveness of the encapsulation system and its impact on the delivery of bioactives within a real food matrix.

2. Materials & Methods

2.1. Materials

Materials for particles and pancakes development: Pectin from citrus peel (galacturonic acid ≥74%) was provided by Sigma-Aldrich (St. Louis, MO, USA), purified zein was from Thermo Scientific (MA, USA). Lime by-products from *Citrus* aurantifolia were kindly supplied by Frubaça Cooperativa de Horticultores (Alcobaça, Portugal). Rice flour and chickpea flour were obtained from Molino Favero (Padova, Italy), soy beverage from Alpro (Ghent, Belgium), baking powder from Selex (Milano, Italy), and granulated sugar. All pancake ingredients were sourced from local markets and certified as gluten-free.

Reagents: DPPH (2,2-diphenyl-1-picrylhydrazyl), Folin & Ciocalteau's reagent, ABTS (2,2'-azino-bis(3-ethylbenzothiazoline-6-sulfonic acid), potassium peroxodisulfate ≥99%, diammonium salt ≥98% and all the digestive salts described by Brodkorb *et al.* (2019) [24] were purchased from Merck-Sigma-Aldrich (Darmstadt, Germany). Potassium dihydrogen phosphate 98%–102% was supplied by Panreac (Barcelona, Spain).

Analytical standards: Gallic acid and chlorogenic acid were supplied by Fluka Chemie AG (Bus, Switzerland); eriocitrin and narirutin were provided to Biosynth Carbosynth (Compton, United Kingdom) and hesperidin was purchased from USP (Twinbrook Pkwy, Rockville, MD, USA). Trolox (6-hydroxy-2,5,7,8-tetramethylchromane-2-carboxylic acid 97%), ferulic acid and rutin were supplied by Merck-Sigma-Aldrich (Darmstadt, Germany). All phenolic standards possessed purities ≥ 98%.

Solvents: Methanol LC-MS grade, methanol HPLC grade, acetic acid HPLC-grade, formic acid 98 – 100% for LC-MS and hydrochloric acid 37% were supplied by Merck (Darmstadt, Germany). Ultrapure water was provided from an Automatic Plus purification system Wasserlab (Navarra, Spain).

In vitro digestion enzymes: α-amylase from Bacillus sp. (50 U/mg solid;), pepsin from porcine gastric mucosa (≥ 250 U/mg solid), porcine bile and pancreatin from porcine pancreas (8 USP; Lipase Activity: ≥ 8 U/mg; Amylase activity: ≥ 100 U/mg; Protease Activity: ≥ 100 U/mg) were provided by Merck-Sigma-Aldrich (Darmstadt, Germany).

2.2. Extraction of phenolics compounds from lime by-products

Phenolic compounds were extracted following the protocol reported by Rodsamran *et al.* (2019)[25] with slight modifications (see Figure S1). Briefly, lime fruit by-products were freeze-dried and pulverized (TM6 Thermomix®, Vorwerk, Wuppertal, Germany) for further extraction using EtOH 50% v/v at a 1:20 ratio w/v. A pretreatment of 10 min was performed in an ultrasounds bath (Branson 5510, Branson Ultrasonic Corp., Danbury, CT, USA) for further 30 min agitation in IKA Eurostar 20 digital (IKA-Werke GmbH & Co, Staufen, Germany). A one-hour decantation step was performed prior to Büchner filtration using Whatman® Grade 1 filter paper. After being stored at −30 °C for 12 hours, the extract was filtered once more prior to ethanol removal using a rotary evaporator (BIBBY sterilin RE200; Stone, UK). Finally, the remained extract was freeze-dried (Lyovapor™ L-200 Pro, BÜCHI Labortechnik AG, Switzerland).

2.3. Microparticles development

2.3.1. Antisolvent precipitation

Antisolvent precipitation was employed to encapsulate lime extract within zein–pectin particles. Initially, lime extract and zein were dissolved in 80% (v/v) EtOH at a 1:100 w/v. The mixture was then centrifuged at 6,000 rpm for 10 minutes at 15 °C (Hettich Universal 320R, HettichLab Technologies, Tuttlingen, Germany). The supernatant was added dropwise to equal volumes of water and then to 0.5% (w/v) pectin solution. The final formulation contained 0.25% (w/v) lime extract, 0.25% (w/v) zein, and 0.25% (w/v) pectin, resulting in a final ethanol concentration of 20% (v/v). The formulation was homogenized using an Ultra-Turrax (IKA T25 digital, IKA-Werke GmbH & Co, Staufen, Germany) at 20,000 rpm for 2 minutes at room temperature. The formulation was further sonicated to reduce particle size (Branson Digital Sonifier Model 450, Marshall

View Article Online
DOI: 10.1039/D6FB00090H

ARTICLE

Table 1. Pancake formulations of the control and increasing percentages of lime particles

Sample	Rice flour (g)	Chickpea flour (g)	Lime flour (g)	Soy beverage (mL)	Baking powder (g)	Sugar (g)
PC	112	38	0	250	10	12
PLP2.5	110	37	4	250	10	12
PLP5	107	36	8	250	10	12

Scientific, Hampton, NH, USA) using a Tapered Microtip 1/8", (101-148-062, amplitude range: 116 – 494 µm) at 50 % amplitude for 10 minutes, applying 30-second pulses on and off (maximum power 120 W). The formulation was centrifuged at 4,000 rpm for 20 min at 15 °C to remove undissolved solids; controls (without lime extract) were prepared using the same procedure.

2.3.2. Spray drying process

Drying conditions were optimized in a Nano Spray Dryer (NSD) (B-90 Büchi Labortechnik AG, Flawil, Switzerland). The NSD's low formulation required, and high yield with minimal material losses facilitated efficient trial-and-error optimization (see Tables S1 and S2). To produce larger quantities of powder for pancake fortification, the lime-loaded formulation was scaled up and dried using a Mini Spray Dryer (MSD) (B-290, Büchi Labortechnik AG, Flawil, Switzerland).

NSD optimisation used the medium mesh (5.5 µm). Formulations were diluted 1:2 v/v with water and dried at 110 °C with a 130 L/min flow. Pump and spray rates were 80%, yielding an outlet temperature of up to 45 °C. Spraying time was limited to 45 min to prevent chamber overheating.

For MSD scale-up, formulations were used undiluted. Spray drying conditions mirrored the NSD optimization: 110 °C inlet, ≤ 55 °C outlet, 60% aspiration, 30% pump rate, and nozzle cleaning frequency set at 5.

2.4. Pancakes development

Pancake batters were mixed in a planetary mixer (Chef XL KVL4100S, KENWOOD, UK) for 3 min at medium speed and 1 min at maximum, then rested 10 min covered. Lime microparticles replaced 2.5% (PLP2.5) or 5% (PLP5) of flour. Formulations were prepared in triplicate, producing ≥15 pancakes per batch (see Table 1).

Batter (~20 mL) was dispensed with a commercial syringe syringe (De Buyer, France; REF: 3358.01) and cooked 1.5 min per side at 200 ± 10 °C on a crepe maker (Krampou, CSRO4AA-KR, France).

For specific gravity, 5 mL of batter was weighed in triplicate to determine bulk density.

2.5. Characterization of formulations and particles

2.5.1. Dynamic light scattering (DLS)

Polydispersity index (PDI), particle size, and ζ-potential were measured using a Malvern Nano ZetaSizer ZS at 25 °C, with the formulation diluted 1:100 in ultrapure water. Five measurements were taken per replicate (≥3).

2.5.2. Thermal analysis

2.5.2.1. TGA & DSC

Thermal gravimetric assay (TGA) was assessed by TGA-DSC (Mettler Toledo TGA-DSC1) using 2 mg of sample, heated from 25 °C to 800 °C at 10 °C/min under N_2, in triplicate. Differential scanning calorimetry (DSC, TA Instruments Q1000) was performed from 10 °C to 300 °C at 10 °C/min under N_2, analysing three replicates.

2.5.2.2. Thermal stability of phenolic compounds

Thermal stability of individual phenolics was evaluated by heating 100 mg of extract and lime-loaded particles at 160 °C and 200 °C (temperatures commonly used in bakery processing) for 2, 5, 10, 20, 30, and 60 min, including 0 min controls, in triplicate. Phenolics were quantified post-heating by HPLC-DAD.

2.5.3. ATR-FTIR

ATR-FTIR was used to assess chemical interactions between wall materials and lime extract. Spectra were recorded on a FTIR-ATR (ATR-PRO ONE, FTIR 4700, Jasco, Tokyo, Japan) with a diamond-composite attenuated total reflectance cell, over 400–4000 cm^{-1}, with 25 scans per sample at 4 cm^{-1} resolution, controlled using Spectra Manager™ v2 software.

2.5.4. SEM determinations

Microparticle morphology was examined via SEM (ZEISS FESEM Ultra Plus) at 3 kV using a secondary detector (SE Everhart-Thornley), with samples mounted on carbon tape and gold-sputtered for ~2 min (Quorum Q150T-S-Plus). Particle size, PDI, and aspect ratio were measured for ≥200 particles using ImageJ v1.53k, according to Silva *et al.* (2022)[26]:

$$\text{Particle aspect ratio (PAR)} = \frac{\text{Particle height}}{\text{Particle length}} \qquad \textit{Eq.1}$$

2.5.5. Encapsulation efficiency, encapsulation yield and payload

Encapsulation efficiency (EE) was calculated as the percentage of lime extract trapped in particles (Eq. 2), encapsulation yield

(EY) as the percentage of total extract relative to the initial formulation (Eq. 3), and payload (PL) as extract content per particle mass (Eq. 4), following Duhoraniman *et al.* (2018)[27] and Wang *et al.* (2014)[28] with minor modifications. Individual phenolics were quantified by HPLC-DAD.

For particle breakage, samples were suspended in 80% EtOH (1:200 w/v), vortexed 2 min at 3,000 g (Wizard IR Vortex, Velp Scientifica, Usmate Velate, Italy), sonicated 2 min, and centrifuged 3 min (Ohaus Frontier™ 5000 series mini centrifuge) to pellet pectin. The supernatant was evaporated under N_2, reconstituted in water to precipitate zein, concentrated 2×, and filtered (0.22 µm PTFE) before HPLC-DAD analysis.

Non-encapsulated extract was measured by suspending particles in acetone (1:100 w/v), followed by vortexing, sonication, centrifugation, evaporation under N_2, 4× reconstitution in water, and filtration.

$$EE\ (\%) = \frac{(Wt - Ws)}{Wt} \times 100 \qquad Eq.2$$

$$EY\ (\%) = \frac{Wt}{Wi} \times 100 \qquad Eq.3$$

$$PL\ (\%) = \frac{Wte}{Wm} \times 100 \qquad Eq.4$$

where *Wt* is the total phenolic mass in particles, *Ws* the surface phenolic mass, *Wi* the theoretical mass of the individual phenolic added, *Wte* the total extract content (from EY), and *Wm* the particle mass. Calculations considered each individual phenolic compound. Determinations were performed in triplicate.

2.6. Pancakes characterization

2.6.1. Proximate composition

The proximate composition was determined in accordance with the guidelines established by Regulation (EU) No 1169/2011 on the provision of food information to consumers [29]. Determinations were performed following the UNE-EN ISO/IEC 17025 standard [30], covering the assessment of energy value, moisture, ash, carbohydrates, total sugars, protein, total dietary fibre (TDF), including its insoluble (IDF) and soluble (SDF) fractions, total and saturated fats, as well as salt and sodium content.

2.6.2. Batter rheology

The rheological analysis was determined by using DRS500 CP4000 PLUS rheometer (Lamy Rheology, France). The batter (~20 mL) was placed in a vessel and warmed until 25 ºC. A MSDIN-11 system was employed following the method described by Bianchi *et al.* (2022)[31]. Shear stress was a function of shear rate over the range of 10 – 300 s^{-1}. The results fitted with the Power-Law model (Ostwald-de Waele relationship), according to the equation:

$$\tau = \mathrm{K} \cdot \gamma^{n} \qquad Eq.5$$

where, τ represents the shear stress (Pa); K, the consistency index (mPa·s) and n the flow index. All measurements were performed in triplicate.

2.6.3. Physicochemical, morphological & colour determinations

Pancakes moisture content was assessed in agreement with AACC method 44-15 A. The water activity (a_w) was determined by utilizing a Hygropalm HC-2AW meter (Rotronic Italia, Milano, Italy) at 25 °C. All analysis were performed at least in triplicate. The weight loss of pancakes was calculated from initial batter and final pancake weights, with ≥ 10 measurements per formulation.

Colour was determined using a Minolta Chroma meter CR-300 (Osaka, Japan) in accordance with CIE-L*a*b* system. *L**-value represents the lightness from 0 to 100; *a** represents greenness-redness and *b**, blueness to yellowness values, ranging both from -127 to 127. Six samples of each batch were measured in four different points. Colour variation was evaluated by calculating the differences between each sample and the control:

$$\Delta E = \sqrt{\Delta L^2 + \Delta b^2 + \Delta a^2} \qquad Eq.6$$

$$\Delta L = (L - L_0)\ ; \Delta a = (a - a_0)\ ; \Delta b = (b - b_0) \qquad Eq.7$$

where, ΔE is the total difference among samples; ΔL, Δa and Δb were the differences between each parameter of the control and samples at different levels of fortification.

Morphological evaluation was determined by measuring the thickness and diameter of the pancakes using a calliper.

2.6.4. Texture evaluation

A texture analyser with a 5-kg load cell (TX-700, Lamy rheology, France) was employed to assess the texture profile analysis (TPA) of pancakes. It was followed the method described by Bruttomesso *et al.* (2024)[32]. Determinations were performed in at least 8 pancakes of each batter batch.

2.6.5. Bioaccessibility and stability of phenolic compounds after *in vitro* digestion

The standardized INFOGEST protocol for static *in vitro* digestion described by Brodkorb *et al.* (2019)[24] was employed to assess phenolic compounds bioaccessibility.

All fluids and enzyme solutions were prepared on the day of analysis to minimize microbial contamination and pH drift. Enzymes and bile salts were kept on ice throughout the procedure to preserve their activity. The entire digestion procedure was performed in a 37 °C water bath with rotary shaking (GFL 1083). To assess phenolic bioaccessibility and matrix effect, 5 g of pancakes were digested, as well as encapsulated and non-encapsulated extract, using equivalent doses (20 mg free extract or 60 mg lime-loaded particles filled until 5 g with water). Test tubes with ultrapure water served as blank controls. All samples were digested in quadruplicate.

To stop enzymatic reactions, samples were transferred to an ice bath. Centrifugation followed at 6,000 rpm for 10 minutes at 10 °C (Hettich Centrifuge Universal 320 R, Tuttlingen, Germany), separating the supernatant and pellet. The supernatant's pH was adjusted to approximately 5.5 to deactivate residual enzymes. Then, 15 mL of the supernatant was freeze-dried and extracted with 5 mL of methanol. The methanolic extract was evaporated under N_2 stream at 40 °C using a RapidVap Vertex Evaporator (Labconco, Kansas City, MO, USA), then reconstituted in water to achieve a 4-fold concentration and filtered through a 0.22 µm PTFE filters. The freeze-dried pellet

View Article Online
DOI: 10.1039/D6FB00090H

ARTICLE

Table 2. Parameters for phenolic compounds quantification by HPLC-DAD and identification through LC-MS/MS.

N	Phenolic compounds	λ_{max} (nm)	R_t (min)	$[M-H]^-$ m/z	Main MS/MS fragments (m/z)	Collision energy (V)	Concentration range (mg/L)	Equation	R_2	LOD (mg/L)	LOQ (mg/L)
1	Gallic acid	278	2.4	169.0	125.0 79.1	- 17 - 27	0.1 – 20	y= 68.67x – 35.08	0.9959	0.05	0.1
2	*p*-hydroxybenzoic acid	278	6.7	137.0	93.0 65.1	- 18 - 31	0.05 – 1	y= 53.75x – 0.21	0.9991	0.025	0.05
3	Chlorogenic acid	325	12.2	353.3	191.1 173.0	- 26 - 24	0.25 – 10	y= 48.28x – 13.70	0.9987	0.1	0.25
4	Ferulic acid	325	17.1	193.0	134.0	-10	0.025 – 10	y= 171.78x – 0.58	0.9999	0.01	0.025
5	Eriocitrin	278	18.1	595.5	286.9 150.7	- 23 - 36	0.1 – 100	y= 44.82x – 13.16	0.9999	0.05	0.1
6	Narirutin	278	21.1	579.1	330.8 482.8	- 28 - 31	0.1 – 20	y= 43.96x – 4.29	0.9968	0.05	0.1
7	Hesperidin	278	22.2	608.9	300.4 285.4	- 26 - 44	0.05 – 100	y= 48.87x + 1.45	0.9999	0.025	0.05
8	Rutin	360	22.8	609.1	299.8 270.7	- 39 - 58	0.1 – 10	y= 38.97x – 7.09	0.9979	0.05	0.1
9	Quercetin	360	24.8	300.9	88.1 70.2	- 23 - 26	0.25 – 20	y= 86.00x – 50.85	0.9960	0.1	0.25

LOD: limit of detection; LOQ: limit of quantification

was subjected to the same extraction process. As a result, both bioaccessible (supernatant) and non-bioaccessible (pellet) fractions were collected for HPLC-DAD analysis, with bioaccessibility measured from the supernatant and recovery calculated by comparing post-digestion content to initial levels.

2.7. Phenolic compounds extraction procedure

To evaluate the initial phenolic compounds content in food samples (lime microparticles and fortified pancakes), the samples were first extracted before analysis.

Lime extract from microparticles was obtained by particles solubilisation at a ratio of 1:100 (w/v) with EtOH 80% (v/v), subjected 10 min UAE and further 30 min agitation at 2,500 rpm (IKA Vibrax VXR Basic, IKA-Werke GmbH & Co, Staufen, Germany). Pancakes were extracted at a ratio of 1:10 (w/v) with MeOH using the same protocol. Samples were centrifuged at 3,500g for 10 min at 10 °C (Hettich Universal 320R, HettichLab Technologies, Tuttlingen, Germany) to separate the supernatant. Freeze-dried lime extract was solubilised at a ratio 1:100 w/v in MeOH. Extracts were diluted or concentrated properly for further analysis. Extractions were performed in triplicate.

2.8. Content in total phenolic, flavonoids & tannins

Total phenolic content (TPC), flavonoids (TFC) and tannins (TTC) were determined by following the methods described by Singleton and Rossi (1965)[33], Herald *et al.* (2012)[34] and Herald *et al.* (2014)[35], respectively and then adapted to microplate by Barbosa-Pereira *et al.* (2018)[36]. Thermo-Fisher microplate photometer (Thermo Scientific™ Multiskan™ FC Microplate Photoreader) for 96-well microplate was used to perform the measurements at 750, 510 and 492 nm, respectively. Gallic acid standard curve was utilized to quantify phenolics in TPC, expressed as mg equivalents of gallic acid (GAE) per g of extract and of particles. Results of TFC and TTC were expressed as mg equivalents of catechin (EC), used for the standard curve, per g of extract and of particles. All assays were performed in triplicate for extract and microparticles.

2.9. Radical scavenging assay

The antioxidant capacity of the lime extract and microparticles was determined by the caption of the radical DPPH following the methodology described by Gadow *et al.* (1997)[37] and adapted to 96-well microplate Barbosa-Pereira *et al.* (2018)[36]. A standard curve of Trolox was accomplished to express the results as mg of Trolox equivalents (TE) per g of extract and of particles. The assays were performed in triplicate.

2.10. Phenolic identity confirmation and quantification through LC-ESI-MS/MS and HPLC-DAD

Following the methodology previously described by Andrade *et al.* (2020)[38], individual phenolics were identified and quantified through HPLC-DAD and their identity was confirmed through LC-MS coupled to electrospray ionization source (ESI), operating in negative mode. Phenolic standards were directly infused into the ion source to assess MS/MS conditions by obtaining the pattern ion $[M-H]^-$ *m/z* and the principal MS/MS fragments. Phenolic compounds identification was further confirmed by

data acquisition in selected reaction monitoring (SRM) mode. Standard stock solutions were diluted to quantify phenolic compounds by the external standard method using at least 6-point standards calibration, at the maximum wavelength of each family group (278, 325 and 360 nm) as described Table 2. Then, individual phenolics were quantified through HPLC-DAD by the external standard method by diluting the stocks solution to obtain at least 6-point standards curves, at the maximum wavelength of each family group (278, 325 and 360 nm).

2.11. Statistical analysis

All analyses were conducted at least in triplicate, and results are presented as mean ± standard deviation. Statistical analysis was performed using IBM® SPSS® Statistics version 29.0.2.0. One-way analysis of variance (ANOVA) was applied, followed by Tukey's post hoc test to determine significant differences, with a significance level set at $p < 0.05$. Effect sizes were calculated and reported as eta squared (η^2) to assess the magnitude of differences. In all cases, 95% confidence intervals were computed and are reported where appropriate.

3. Results & Discussion

3.1. Formulation characterization

Particle size, PDI and ζ-potential are shown in Table 3.

Antisolvent precipitation produced zein nanoparticles of 140.36 nm (control) and 177.90 nm (lime-loaded), with positive ζ-potentials of +9.27 mV and +24.61 mV, respectively. The cationic charge arises from the aqueous pH (~5.5) being below zein's isoelectric point (pI = 6.2), causing protein protonation [39]. The incorporation of lime extract further decreased the pH, thereby enhancing nanoparticle stability and increasing particle size [40].

Adding zein nanoparticles to pectin additionally increased particle size to 389.38 nm (control) and 361.48 nm (lime-loaded), which can be ascribed to the high molecular weight and degree of esterification of pectin. The incorporation of pectin promotes interactions with zein, while the presence of encapsulated bioactives influences particle assembly, thus modulating their final size [41].

Table 3. Particle size, ζ-potential and PDI of liquid formulations.

	Control	Lime-loaded	η^2	Sig.
Zein nanoparticles				
Particle size (nm)	140.36 ± 4.06	177.90 ± 1.57	0.98	***
PDI	0.13 ± 0.03	0.08 ± 0.02	0.50	*
Zeta potential (mV)	9.27 ± 1.46	24.61 ± 0.78	0.98	***
Pectin-zein nanoparticles				
Particle size (nm)	389.38 ± 3.84	361.48 ± 6.92	0.89	***
PDI	0.09 ± 0.02	0.07 ± 0.02	0.30	n.s.
Zeta potential (mV)	-62.48 ± 2.63	-39.75 ± 0.66	0.98	***

PDI: polydispersity index. Statistical significance: ***p <0.001; **p <0.01; *p <0.05; and n.s. =not significant (p >0.05).

With pectin incorporation, ζ-potential shifted to negative (-62.48 mV control, -39.75 mV lime-loaded) due to ionization of pectin's carboxyl groups (pKa 3.5), indicating core–shell formation via electrostatic adsorption onto zein nanoparticles [42].

All formulations showed a homogeneous size distribution, with polydispersity index (PDI) values ≤ 0.1, indicating minimal particle aggregation and lower variability than other reported for zein–pectin particles[13]. This uniformity is due to steric repulsion from the pectin coating, which effectively prevents aggregation [13,43].

3.2. Particles characterization

3.2.1. Micro-structure analysis

The morphology and size of the produced dried microparticles determined through SEM are shown in Table 4 and Figure 1.

Nanosprayed particles obtained from the control and lime-loaded formulations have shown diameters of 0.62 ± 0.27 µm, and 0.70 ± 0.30 µm, respectively. These particle sizes reflect the combined influence of formulation composition and nanospray-drying parameters, particularly mesh size and polymer interactions, which rule droplet formation, solvent evaporation, and final particle consolidation [44]. Both control and lime-loaded nanosprayed microparticles exhibited a spherical shape, as confirmed by particle aspect ratio results close to 1, with lime-loaded particles displaying a smoother surface to the control ones [45].

Nano-sprayed microparticles provided a high PDI of approximately 0.66 for both control and lime-loaded microparticles. This elevated polydispersity can be attributed to the nanospray-drying process itself, where electrostatic forces during particle collection, combined with the presence of highly charged macromolecules such as proteins and polysaccharides, promote heterogeneous droplet breakup and particle formation, ultimately leading to wider size distributions [18,46].

As expected, MSD produced larger microparticles, about twice the previous size, without affecting PDI or aspect ratio.

3.2.2. FTIR

Infrared spectroscopy was employed to assess the influence of the drying process in materials chemical interactions (Figure 2). The pectin spectrum revealed characteristic peaks of carbohydrates. Peaks allocated to O–H (3500 to 3000 cm^{-1}) are mainly attributed to galacturonic acid inter- and intra-molecular H-bonds. C–H stretching vibrations are assigned to 3000-2900 cm^{-1} region. Peaks associated to the esterified carbonyl groups (C=O) are represented at 1730 cm^{-1}. The COO^- stretching vibration are depicted at 1615 cm^{-1}. The peak at 1224 cm^{-1} was associated with the C-OH stretching vibrations in the branched chains. The absorption bands observed between 1200 and 850 cm^{-1}, characteristic of polysaccharides, correspond to CH_2 deformation as well as C–O and C–C stretching vibrations. Indeed, the peak at 1010 cm^{-1} was related to the C–O stretching vibration bond, representing glycosidic bound. The band at 1225 cm^{-1} corresponds to CH_3CO stretching, while the absorption at 1145 cm^{-1} is attributed to C–O–C stretching vibrations of glycosidic linkages [13,47,48]. Freeze-dried lime extract

View Article Online
DOI: 10.1039/D6FB00090H

ARTICLE

Table 4. Encapsulation and morphological determinations of both control and lime-loaded particles.

	Microparticles (NSD)		Lime-loaded microparticles (MSD)	η^2	Sig.
	Control	Lime-loaded			
Encapsulation efficiency (%)	n.a.	80.72 ± 6.44	82.64 ± 7.77	0.23	n.s.
Encapsulation yield (%)	n.a.	94.38 ± 9.20	91.75 ± 10.44	0.21	n.s.
Payload (%)	n.a.	31.46 ± 3.07	30.58 ± 3.48	0.26	n.s.
Particle diameter (µm)	0.62 ± 0.27^{c}	0.70 ± 0.30^{b}	1.61 ± 0.70^{a}	0.49	***
PDI	0.66 ± 0.01	0.65 ± 0.00	0.66 ± 0.01	0.52	n.s.
Particle aspect ratio	1.03 ± 0.11	1.02 ± 0.10	1.03 ± 0.30	0.00	n.s.

n.a.: not apply. Statistical significance: ***p <0.001; **p <0.01; *p <0.05; and n.s. = not significant (p >0.05). Lowercase letters indicate statistical differences horizontally

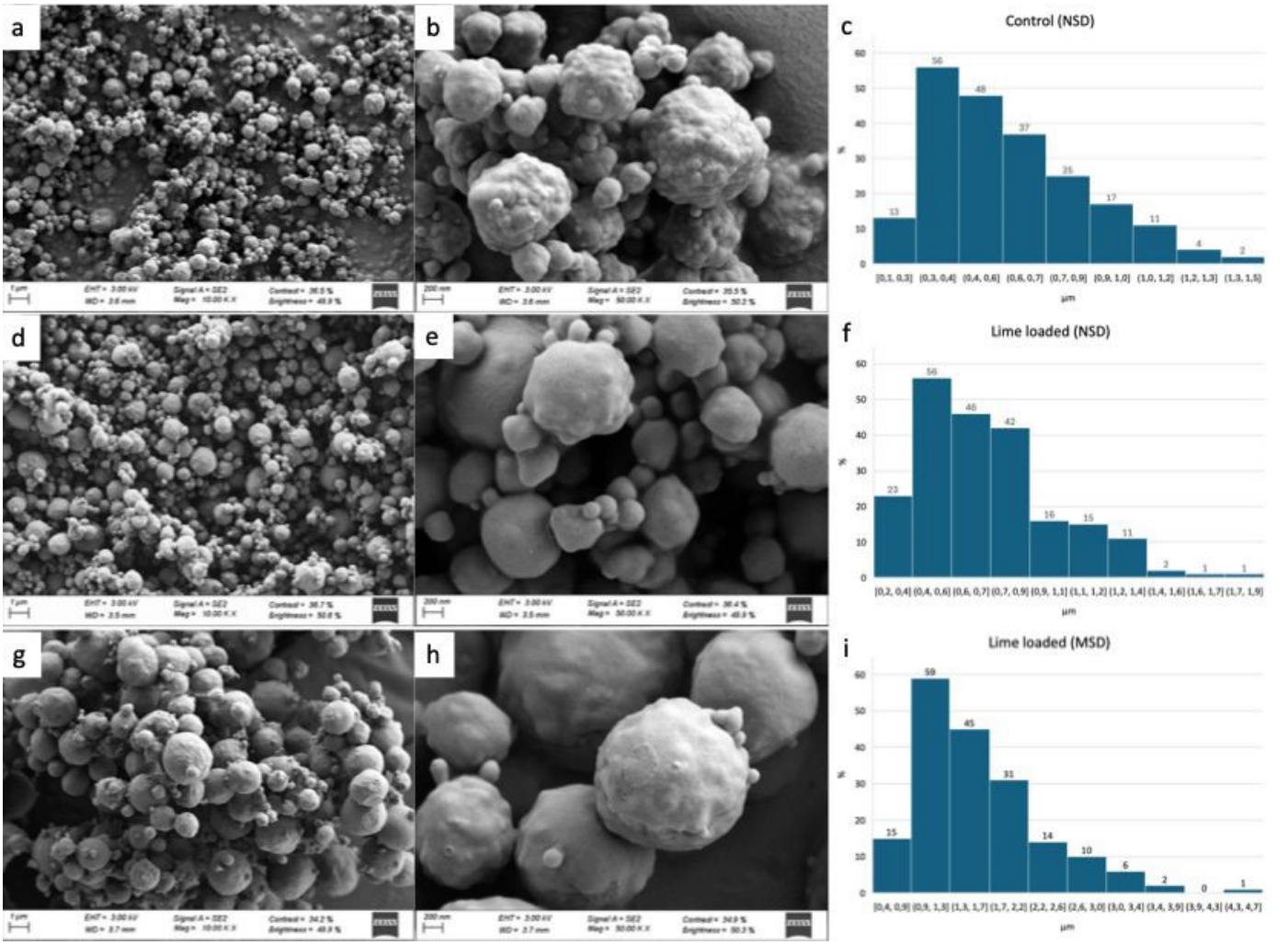

Figure 1. SEM images of: 1st line nanosprayed control particles at 10x (a), 50x (b) and particle size distribution (c). 2nd line, lime-loaded nanosprayed particles at 10x (d), 50x (e) and particle size distribution (f). 3rd line corresponds to lime loaded minisprayed particles at 10x (g), 50x (h) and particle size distribution (i).

View Article Online
DOI: 10.1039/D6FB00090H

ARTICLE

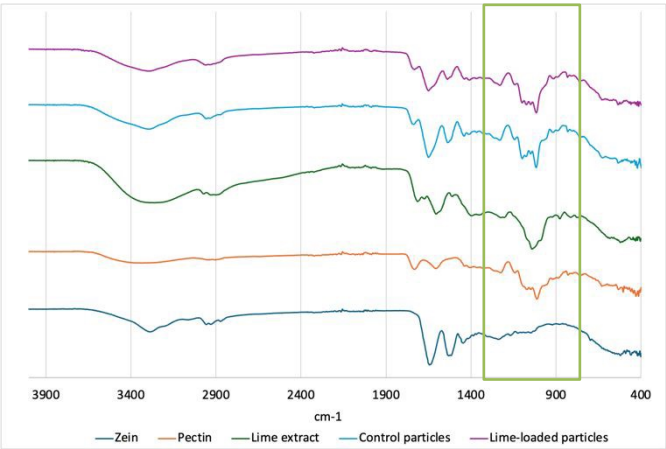

Figure 2. Normalized FTIR spectra of wall and core materials, and both control and lime-loaded nanosprayed microparticles. The region with the main differences is represented by a green square.

has shown a deep O–H peak (3500 – 3000 cm^{-1}), due to its hygroscopic nature. Additionally, the extract shared the prominent band peaks observed for pectin, considering some remaining pectin and other glycosides content after lime by-products extraction.

Zein spectrum revealed protein characteristic absorption bands of Amide I, Amide II and Amide III, representing as the strongest peaks at 1645 cm^{-1}, 1510 cm^{-1} and 1444 cm^{-1}, related to C=O stretching, N–H bending and C–H vibrational band, respectively [13].

The successful incorporation of all components in both control and lime-loaded particles was confirmed by the presence of characteristic bands from each material in their respective spectra, while no new absorption bands were noticed. Peaks corresponding to Amide I and Amide II from zein were observed in both particles, although in lime-loaded were less intense. Moreover, the vibration of the carbonyl group of pectin (1730 cm^{-1}) was also found. The region between 1400 and 1000 cm^{-1}, associated with aliphatic and aromatic fractions of amino acid groups, showed the most prominent differences among the samples. Notably, this region also includes C–H vibrations at 1230 cm^{-1}, as well as –CH and –OH stretching from aromatic rings and glycosidic linkages present in pectin and lime extract.

3.2.3. Thermal analysis

3.2.3.1. TGA & DSC

TGA-DTG and DSC thermograms are represented in Figure 3 and Figure 4, respectively.

A similar degradation pattern was observed for both types of particles, which presented various thermal decomposition events within 25–800 °C, as presented TGA results.

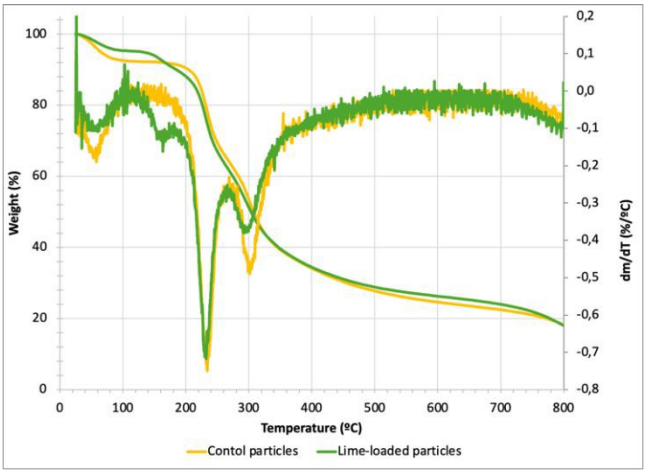

Figure 3. TGA-DTG thermograms of control and lime-loaded particles.

Thermograms could be divided into three main regions: 25 – 210 °C, 210 – 400 °C, and 400 – 800 °C. The first event is related to water evaporation absorbed in particles, as represented by an 8% weight loss for control particles, whereas for lime-loaded particles just accomplished at 5% [49]. The second and most significant degradation event occurred between 200 and 400 °C, with a sharp weight loss peaking at approximately 230 °C, accounting for around 65% of the total mass loss. This stage represents pectin pyrolytic decomposition, where galacturonic acid chains undergo extensive thermal degradation followed by decarboxylation of the main chains [50]. Moreover, it was observed a degradation peak at 300 °C, corresponding to zein degradation [51]. In the last degradation stage, the weight slowly lost until remain a 20% of initial weight, attributed to the thermal decomposition of non-volatile residues, such as char [50].

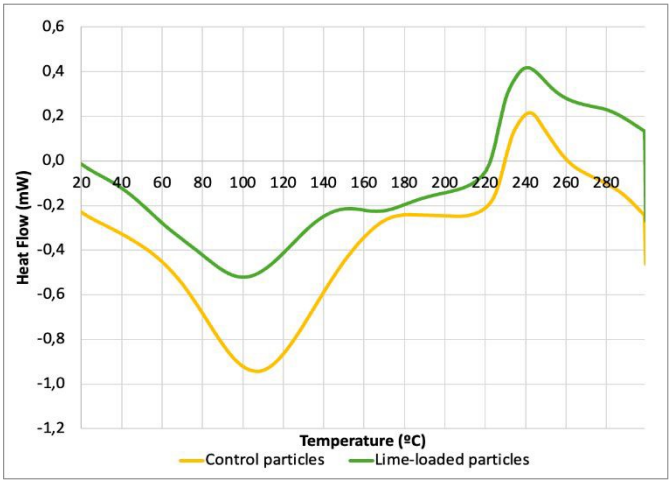

Figure 4. DSC thermograms of control and lime-loaded particle.

View Article Online
DOI: 10.1039/D6FB00090H

ARTICLE

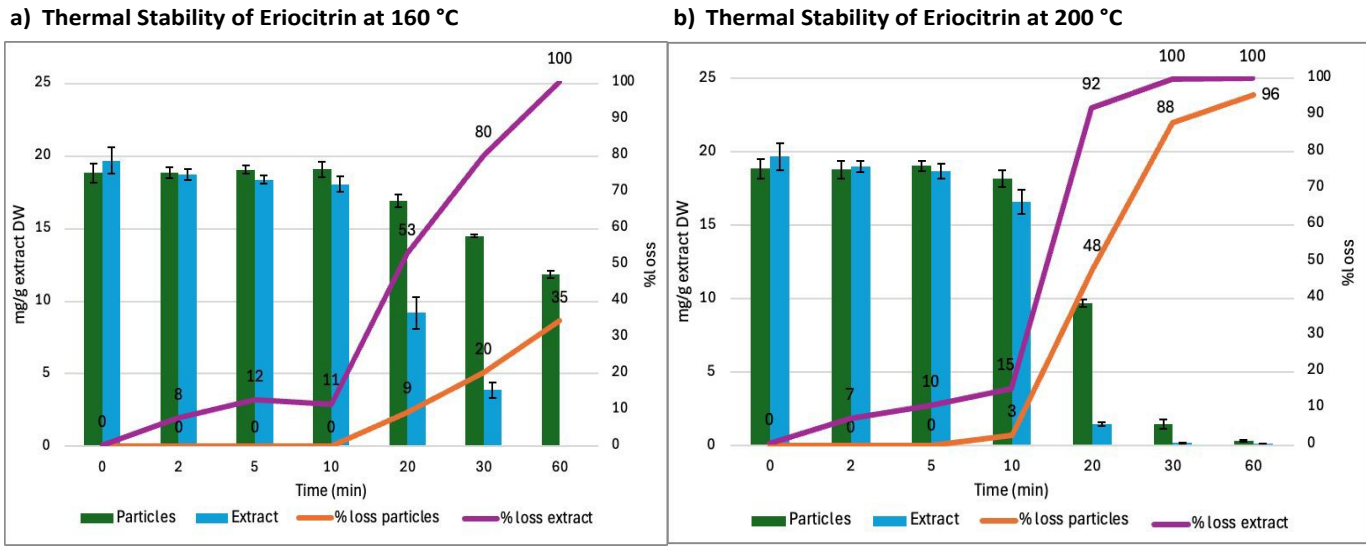

Figure 5. Quantification of eriocitrin in both the free extract and encapsulated particles after being subjected to thermal stability analysis. a) shows results after exposure to 160 °C, and b) to 200 °C. Reported loss percentages represent the average degradation observed over time for the main flavanone glycosides (eriocitrin, narirutin, and hesperidin).

Thermal transitions of both control and lime-loaded particles were assessed through DSC, which thermograms revealed similar trends. Both control and lime-loaded nanoparticles have displayed a maximum, broad endothermic peak at 110 °C and 100 °C, respectively, attributed to water evaporation. The second exothermic peak at 240 °C was related to degradation event [52].

The main endothermic peak in control particles shown in Figure 4 overlaps with other thermal transitions, including the glass transition temperature (T_g) of zein, which has been reported by several authors to occur between 150 and 180 °C [13]. In contrast, lime extract–loaded particles exhibited a more distinct endothermic peak at approximately 170 °C, which can be attributed to the T_g of zein, suggesting a clearer manifestation of this transition in the presence of the extract. As observed in TGA analysis, the main thermal degradation event occurred at approximately 230 °C.

3.2.3.2. Phenolic compounds thermal stability

Thermal stability of individual phenolics was assessed by their quantification after heating exposure. Figure 5 represents eriocitrin degradation pattern, as the main phenolic compound found in lime-extract barely presented in citrus pectin used for particles development. At 160 °C, 20 min caused 53% eriocitrin degradation in free extract versus 9% in particles; after 30 min, 80% vs. 20%; and after 1 h, 100% vs. 35%. At 200 °C, after 10 min, 15% of free extract degraded vs. 3% encapsulated; after 20 min, 92% vs. 48%; and after 30 min, 100% vs. 88%.

Therefore, encapsulation strongly protected the extract against heat degradation, maintaining stability up to 30 min at 200 °C and over an hour at 160 °C, demonstrating suitability for heat-processed foods.

3.2.4. Encapsulation efficiency, yield and payload

The lime by-product extract was successfully encapsulated in zein–pectin microparticles, with EE, EY, and PL are shown in Table 4. A high EE of 82.64 ± 7.77% was obtained, due to the strong encapsulating capacity of zein and pectin. This, together with the preserved eriocitrin levels in the thermal stability tests, indicates effective protection of the extract. The payload (30.58 ± 3.48%) was close to the theoretical 33.33% based on the core-to-wall ratio, and the EY (91.75 ± 10.44%) reflected minimal extract loss.

When comparable definitions of EE, EY and PL are considered, the results shown in Table 4 generally fall within similar ranges or are slightly superior [13,53,54]. This highlights the improved performance of the developed zein–pectin system in terms of bioactive retention and process efficiency.

3.2.5. Lime extract and microparticles phenolic composition and antioxidant properties

Lime extract and microparticles were characterized for TPC, TFC, TTC, and DPPH radical-scavenging activity, and individual phenolics were quantified by HPLC-DAD. Results are shown in Table 5.

Lime extract presented TPC value of 31.30 ± 1.25 mg GAE/g extract, TFC of 8.85 ± 0.51 mg CE/g and TTC of 2.10 ± 0.40 mg

View Article Online
DOI: 10.1039/D6FB00090H

ARTICLE

Table 5. Total phenolic, flavonoid and tannin content; antioxidant properties and phenolic compounds quantification in lime extract and developed microparticles.

	Lime extract	Microparticles (NSD)		Lime-loaded microparticles (MSD)	η^2	Sig.
		Control	Lime-loaded			
Total phenolics & antioxidant composition						
TPC (mg GAE/g)	31.30 ± 1.25	10.42 ± 0.18^{c}	19.22 ± 0.26^{a}	18.45 ± 0.19^{b}	0.99	***
TFC (mg CatE/g)	8.85 ± 0.51	0.16 ± 0.03^{c}	3.01 ± 0.03^{a}	2.66 ± 0.05^{b}	0.99	***
TTC (mg CatE/g)	2.10 ± 0.40	< LOD	0.44 ± 0.04	0.36 ± 0.01	0.99	***
DPPH (mg TE/g)	19.69 ± 0.85	3.55 ± 0.12^{b}	6.06 ± 0.04^{a}	6.51 ± 0.35^{a}	0.98	***
Phenolic compounds (mg/g)						
Gallic acid	5.23 ± 0.21	< LOD	1.68 ± 0.02	1.52 ± 0.02	0.97	***
4-hydroxybenzoic acid	0.11 ± 0.01	< LOD	0.02 ± 0.001	0.02 ± 0.001	0.33	n.s.
Chlorogenic acid	0.40 ± 0.11	< LOD	0.10 ± 0.002	0.10 ± 0.01	0.20	n.s.
Ferulic acid	1.80 ± 0.01	< LOD	0.53 ± 0.003	0.65 ± 0.02	0.99	***
Eriocitrin	16.71 ± 1.39	0.07 ± 0.001^{b}	4.84 ± 0.11^{a}	5.00 ± 0.09^{a}	0.99	***
Narirutin	4.15 ± 0.62	0.07 ± 0.001^{c}	1.15 ± 0.007^{b}	1.37 ± 0.02^{a}	0.99	***
Hesperidin	19.95 ± 1.22	1.56 ± 0.03^{b}	6.63 ± 0.01^{a}	6.49 ± 0.19^{a}	0.99	***
Rutin	2.22 ± 0.09	< LOD	0.59 ± 0.003	0.56 ± 0.02	0.63	n.s.
Quercetin	4.86 ± 1.17	< LOD	1.43 ± 0.005	1.48 ± 0.06	0.32	n.s.

Statistical significance: ***p <0.001; **p <0.01; *p <0.05; and n.s. = not significant (p >0.05).

CE/g. The extract yielded from lime by-products displayed antioxidant properties assessed through DPPH radical reduction of 19.69 ± 0.85 mg TE/g extract.

Both control and lime-loaded microparticles were characterized. The citrus-derived pectin contained residual phenolics, which contributed to spectrophotometric signals and HPLC-DAD quantification [55]. Even so, lime-loaded particles consistently showed higher values than controls.

Specifically, the functionalized particles attained 19.22 ± 0.26 mg GAE/g for TPC, and 3.01 ± 0.03 mg CE/g for TFC. TTC values were low (0.44 ± 0.04 mg CE/g particles), and undetectable in control particles. Lime-loaded particles showed nearly double the antioxidant activity of controls, reaching 6.06 ± 0.04 mg TE/g. Overall, both the extract and microparticles confirmed a strong flavonoid contribution, representing about 30% of total phenolics (see Table 5).

Table 2 presents the LC-ESI-MS/MS identification parameters and validation data, confirming the identification of ten phenolic compounds. HPLC-DAD quantification displayed in Table 5 revealed phenolics belonging to different structural classes: benzoic acid derivatives (gallic acid and *p*-hydroxybenzoic acid), hydroxycinnamic acids (chlorogenic acid and ferulic acid), flavanone glycosides (eriocitrin, narirutin, and hesperidin), flavonol glycosides (rutin) and flavonols (quercetin). Flavanone glycosides were the main phenolic subclass found in in lime by-product extract, highlighting hesperidin and eriocitrin as the predominant compounds (19.95 ± 1.22 mg/g extract, 16.71 ± 1.39 mg/g extract, respectively). Moreover, gallic acid was measured at 5.23 ± 0.21 mg/g extract and quercetin at 4.86 ± 1.17 mg/g extract. Control microparticles also showed some quantifiable phenolic compounds, particularly hesperidin, eriocitrin and narirutin, attributed to phenolics entrapped within the pectin matrix.

In agreement with the obtained phenolic quantification results, Esparza-Martínez *et al.* (2016)[56] reported hesperidin and eriocitrin as the main phenolics in fresh lime waste, and observed similar antioxidant activity. Similarly, Mateus *et al.* (2024)[23] identified flavanone derivatives as predominant, though they found eriocitrin—not hesperidin—as the major compound.

Standardizing extraction and purification processes, along with thorough extract characterization, is essential due to the many factors that influence chemical composition—such as climate, cultivar, and maturity stage. These variables also affect antioxidant properties, which are critical for using extracts in food applications. This variability challenges the valorisation of agri-food by-products and hinders comparisons across studies.

3.2.6. Nano and mini spray production. Scale-up comparison

For fortifying gluten-free and vegan pancakes, a large quantity of microparticles was needed. While the NSD is suitable for optimization due to low sample volume, its limited throughput hindered scalability. NSD achieved a high recovery of 93.43 ± 1.71 % but had a low drying rate (1.21 ± 0.13 mL/min; effective throughput 0.60 ± 0.07 mL/min due to required dilution).

Scaling up with the Mini-Spray Dryer MSD allowed higher throughput without dilution, maintaining drying conditions at 110 °C inlet and ≤ 55 °C outlet. The MSD achieved a drying rate of 8.17 ± 1.02 mL/min and 57.20 ± 8.59 % recovery. Despite lower recovery than NSD, production efficiency improved by 87%, providing a practical solution for larger-scale production.

Microparticles produced with MSD showed larger diameters but similar PDI and aspect ratios. Antioxidant activity, total phenolic content, and individual phenolics remained largely comparable to NSD particles, with six of the nine quantified phenolics showing no significant differences. Minor variations were observed, with gallic acid slightly lower and ferulic acid and narirutin slightly higher. Encapsulation efficiency, yield, and payload were unaffected (see Table 4, Table 5 and Figure 1).

The results confirm that bioactive compounds were preserved during scale-up, supported by thermal stability data (see Section 3.2.3. and Figure 5). NSD is thus effective for initial development, with MSD enabling scalable production of functional ingredients for food applications.

3.3. Pancakes characterization

3.3.1. Proximate composition

The proximate composition of control and fortified pancakes is shown in Table 6.

Macronutrient levels remained similar across all formulations. Carbohydrates decreased slightly in PLP5 (from 36.30 to 33.7 g/100 g). Both fortified samples showed a reduction of approximately 70% in total sugars, reaching < 1.5 g/100 g. All pancakes contained < 3 g/100 g total fat and < 1.5 g/100 g saturated fat, allowing the nutritional claims "low in sugars," "low in fat," and "low in saturated fat" under Regulation (EU) No. 1924/2006 [57].

PLP2.5 did not significantly increase total dietary fibre (TDF) compared to the control (1.3 g/100 g), whereas PLP5 showed a clear rise to 2.7 g/100 g. Insoluble fibre followed the same trend, increasing from 0.3 g/100 g in the control to 0.9 g/100 g in PLP5.

Although the microparticles contained pectin (a soluble fibre), the non-selective extraction of lime by-products likely introduced insoluble fibre from the peel, explaining the higher insoluble fraction content [58]. This observed fibre increase has also been reported by other authors when fortifying bakery products with plant extracts [59]. The enhancement of insoluble fibre is related to health promoting effects, as it is associated with improved insulin sensitivity, reduced type 2 diabetes risk, and enhanced gut health [60,61].

3.3.2. Specific gravity and rheological properties of batters

Specific gravity and batter rheology are closely related parameters that affect the texture of the final baked product.

Table 7 shows a decrease in the specific gravity with increasing concentrations of lime-loaded microparticles, dropping from 1.06 ± 0.01 in the control pancake to 0.86 ± 0.04 in PLP5. This reduction is attributed to the presence of pectin, a gelling and a stabilizing agent commonly used in bakery products. Its ability to lower the surface tension of the aqueous phase promotes

Table 6. Proximate composition of developed pancakes.

	PC	PLP2.5	PLP5	η^2	Sig.
Energy Kcal/100 g	191.33 ± 16.26	189.47 ± 3.44	181.37 ± 6.65	0.21	n.s.
Total fat g/100g FW	1.80 ± 0.01^{ab}	1.87 ± 0.05 ^{a}	1.72 ± 0.04^{b}	0.81	**
Saturated fat g/100g FW	0.29 ± 0.01	0.31 ± 0.02	0.29 ± 0.03	0.13	n.s.
Carbohydrate g/100g FW	36.30 ± 0.39^{a}	36.41 ± 0.34^{a}	33.56 ± 0.59^{b}	0.93	***
Total sugars g/100g FW	4.56 ± 0.22^{a}	1.20 ± 0.14^{b}	1.40 ± 0.07^{b}	0.96	***
Protein g/100g FW	6.44 ± 0.46	6.0 ± 0.62	6.4 ± 0.43	0.56	n.s.
Salt g/100g FW	1.10 ± 0.15	1.098 ± 0.05	1.02 ± 0.12	0.51	n.s.
Sodium g/100g FW	0.44 ± 0.03	0.44 ± 0.02	0.41 ± 0.03	0.46	n.s.
TDF g/100g FW	1.53 ± 0.13^{b}	1.11 ± 0.15^{b}	2.72 ± 0.22^{a}	0.96	***
IDF g/100g FW	1.30 ± 0.18^{b}	1.0 ± 0.13^{b}	1.92 ± 0^{a}	0.91	***
SDF g/100g FW	< 1.0	< 1.0	< 1.0	n.a.	n.a.
Ash g/100g FW	2.70 ± 0.03^{b}	2.93 ± 0.08^{a}	2.71 ± 0.04^{b}	0.86	**

Statistical significance: ***p <0.001; **p <0.01; *p <0.05; and n.s. = not significant (p >0.05).

greater air incorporation during mixing, contributing to the observed decrease in specific gravity [62,63].

Batter consistency is a key property affecting product volume, as higher viscosity improves air retention and loaf height.

In this study, the consistency index (K) increased from 11.06 ± 1.09 Pa·s in the control (PC) to 21.77 ± 1.14 Pa·s in PLP5, while PLP2.5 showed no difference (see Table 7).

Low-consistency batters, like the control, entrapped less air and produced lower-volume products [64]. In contrast, the addition of lime-loaded microparticles significantly increased cake height, indicating enhanced air incorporation and batter structure (see Table 8). This effect is ascribed to the increased batter viscosity imparted by dietary fibres, which hydrate and restrict flow, thereby improving air retention during mixing and baking [65].

Table 7. Rheology and specific gravity of batters.

Samples	Specific gravity	Rheology		
		Flow index (n)	Consistency (k) (Pa·s)	R^2
PC	1.06 ± 0.01^{a}	0.27 ± 0.01^{c}	11.06 ± 1.09^{b}	0.94 ± 0.01^{b}
PLP2.5	0.96 ± 0.02^{b}	0.40 ± 0.02^{b}	11.95 ± 0.95^{b}	0.99 ± 0.00^{a}
PLP5	0.86 ± 0.04^{c}	0.44 ± 0.01^{a}	21.77 ± 1.14^{a}	0.99 ± 0.00^{a}
η^2	0.94	0.97	0.95	0.93
Sig.	***	***	***	*

Statistical significance: ***p <0.001; **p <0.01; *p <0.05; and n.s. = not significant (p >0.05).

View Article Online
DOI: 10.1039/D6FB00090H

ARTICLE

Table 8. Morphological, water-related, textural, colour properties and phenolic composition of pancakes fortified with increasing levels of lime particles.

Parameters		PC	PLP2.5	PLP5	η^2	Sig.
Morphological	Height (cm)	0.80 ± 0.09^b	0.94 ± 0.04^a	0.97 ± 0.09^a	0.49	**
	Diameter (cm)	7.25 ± 0.29^a	6.96 ± 0.15^b	6.35 ± 0.12^c	0.49	***
	Spread ratio	9.14 ± 1.16^a	7.45 ± 0.43^b	6.57 ± 0.49^c	0.67	***
Water-related	a_w	0.960 ± 0.007	0.960 ± 0.01	0.960 ± 0.003	0.01	n.s.
	Moisture (%)	49.62 ± 2.33^b	52.44 ± 1.04^a	52.76 ± 1.73^a	0.42	**
	Weight loss (%)	6.88 ± 1.07^a	3.04 ± 0.37^b	3.48 ± 0.73^b	0.83	***
Texture	Cohesiveness	0.80 ± 0.03^a	0.75 ± 0.03^b	0.73 ± 0.01^c	0.62	**
	Gumminess (N)	4.40 ± 0.92^c	5.93 ± 0.39^b	8.35 ± 0.96^a	0.81	***
	Chewiness (N)	4.47 ± 0.94^c	6.04 ± 0.40^b	8.51 ± 0.98^a	0.81	***
	Hardness (N)	5.00 ± 1.13^c	8.56 ± 0.71^b	12.48 ± 1.58^a	0.87	***
Colour	L*	71.62 ± 2.75^a	69.19 ± 2.86^b	63.80 ± 4.28^c	0.60	***
	a*	5.47 ± 1.62^c	6.55 ± 1.34^b	11.25 ± 2.08^a	0.68	***
	b*	38.39 ± 2.11^b	40.85 ± 4.09^a	40.40 ± 1.33^a	0.12	**
	ΔE	n.a.	6.56	49.25	n.a.	n.a.
Phenolic compounds	Chlorogenic acid (µg/g)	-	3.03 ± 0.08	3.94 ± 0.34	0.83	*
	Ferulic acid (µg/g)	-	3.32 ± 0.06	6.69 ± 0.31	0.99	***
	Eriocitrin (µg/g)	-	24.05 ± 0.15	51.52 ± 3.71	0.98	***
	Narirutin (µg/g)	-	12.26 ± 0.18	22.88 ± 1.28	0.98	***
	Hesperidin (µg/g)	-	73.65 ± 0.84	147.30 ± 5.95	0.99	***
	Rutin (µg/g)	-	5.00 ± 0.02	9.18 ± 0.76	0.96	***

Statistical significance: ***p <0.001; **p <0.01; *p <0.05; and n.s. = not significant (p >0.05).

a) Lime extract b) Lime-loaded microparticles c) PC d) PLP2.5 e) PLP5

Figure 6. From the left to the right, images of the freeze-dried lime by-product extract (a), lime-loaded microparticles (b), and all the developed pancakes (PC (c), PLP2.5 (d), and PLP5 (e)).

View Article Online
DOI: 10.1039/D6FB00090H

ARTICLE

On the other hand, the flow index increased from 0.27 ± 0.01 in the control pancake to 0.44 ± 0.01 in the PLP5 formulation. Despite the increase in flow index, all batters exhibited shear-thinning behaviour, as described by the Ostwald–de Waele model, indicating that their viscosity decreased with increasing shear rate [66].

However, the increased flow index at higher fortification indicates reduced shear-thinning, likely due to the added viscosity from lime-loaded microparticles. This rheological change may have enhanced air retention during mixing, contributing to the higher pancake volume observed (see Table 8).

3.3.3. Physicochemical, morphological and colour properties

Table 8 reported pancakes' Lab colour code and total colour differences, morphological, water-related determinations, texture profile analysis and the individual phenolic content in each pancake formulation.

Moisture increased from 49.62 ± 2.33% in the control to 52.44 ± 1.04% (PLP2.5) and 52.76 ± 1.73% (PLP5). This rise reflects the uniform baking time and the higher fibre content, which enhances water absorption and retention [67].

Water activity, as an indicator of shelf-life and microbial stability, was identical across all pancakes (aw = 0.96).

Regarding morphology, the incorporation of lime-loaded microparticles significantly increased pancake height and reduced diameter, consistent with the batter's rheological behaviour (Section 3.3.2.). As a result, the spread ratio decreased from 9.14 ± 1.16 (PC) to 6.57 ± 0.49 (PLP5). The thicker structural matrix limited moisture evaporation during baking, directly contributing to the observed increase in moisture content. Consequently, weight loss dropped markedly from 6.88 ± 1.07 % in the control to 3.04 ± 0.37 % (PLP2.5) and 3.48 ± 0.73 % (PLP5).

Food colour plays a decisive role in consumer perception, and fortification markedly altered the visual attributes of the pancakes. As shown in Figure 6 and Table 8, fortified pancakes displayed significant colour changes, characterized by a slight reduction in lightness that imparted a more toasted appearance. The a* value increased substantially, from 5.47 ± 1.62 (PC) to 11.25 ± 2.08 (PLP5), resulting in a visibly redder hue, while b* values showed minor increases. Consequently, the total colour difference reached 6.56 in PLP2.5 and 49.25 in PLP5, confirming that fortification produced clearly perceptible colour shifts toward red and, to a lesser extent, yellow tones.

Importantly, encapsulation effectively modulated the visual impact of the lime extract by masking its inherent green colour (Figure 6), which would otherwise be undesirable in bakery products. Given that colour preferences are strongly shaped by familiarity and cultural expectations, this masking effect is particularly relevant, as it may enhance consumer acceptance in markets where green-coloured baked goods are uncommon or perceived negatively [68].

The encapsulation strategy not only preserved functionality but also enabled colour adjustments compatible with consumer expectations, reinforcing its suitability for food fortification applications.

3.3.4. Texture evaluation

Textural profile analysis (TPA) results (Table 8) revealed that fortification induced measurable modifications in pancake texture. Cohesiveness decreased slightly with fortification, from 0.80 (PC) to 0.75 ± 0.03 (PLP2.5) and 0.73 ± 0.01 (PLP5). Hardness increased notably, from 5.00 ± 1.13 N in PC to 8.56 ± 0.71 N and 12.48 ± 1.58 N in PLP2.5 and PLP5, respectively. As direct consequence, gumminess and chewiness also rose, reaching 8.35 ± 0.96 N and 8.51 ± 0.98 N in PLP5. Both parameters were strongly correlated with hardness (r = 0.997), while cohesiveness showed a negative correlation (r = – 0.965), indicating that fibre-driven structural reinforcement governed the observed textural changes.

Increases in hardness are consistent with the incorporation of fruit- and vegetable-derived by-products, which raise fibre content and reinforce the matrix structure [697069,70]. Importantly, pancake hardness remained well below that reported for rice-based gluten-free pancakes enriched with hydrocolloids (up to 30 N) [71]. Moreover, the fortified pancakes exhibited hardness and cohesiveness comparable to wheat-based controls, indicating that lime-loaded microparticles contributed to gluten-like textural properties and enhanced product quality.

3.3.5. Phenolic compounds *in vitro* bioaccessibility

Phenolic compounds undergo biotransformation during *in vitro* digestion, influenced by delivery form, encapsulating materials, and food matrix, which affect bioaccessibility. Digestion was performed on pancakes, particles, and extract separately to assess matrix effects. Quantification results of the main phenolic compounds, their bioaccessibility and recoveries are presented in Figure 7.

Encapsulation improved bioaccessibility and recovery of lime extract phenolics by at least 10% compared to the non-encapsulated form. Chlorogenic acid, narirutin, and hesperidin remained nearly 100% bioaccessible and fully recovered, while rutin showed some degradation but ~90% of recovered rutin remained bioaccessible.

The lime extract was not further purified, thereby contained phenolics and co-extracted pectin, which protected the polyphenols during freeze-drying. As a result, pectin

View Article Online
DOI: 10.1039/D6FB00090H

contributed to enhanced non-encapsulated extract stability and ultimately improved the bioaccessibility of phenolic compounds similarly to the lime-load particles. [72]Under acidic conditions, pectin-based particles shrank and aggregated due to $–COO^-$ deprotonation, which restricted the release. In contrast, at neutral pH, particle swelling induced more gradual release of phenolics, thereby improving their bioaccessibility [72].

Apart from the effect of pectin, zein also contributed to maintaining extract stability and controlled release, supporting the high polyphenol bioaccessibility observed in Figure 7 [73]. In zein–pectin particles, the release of the core material predominantly occurred in the small intestine. The delayed release is attributed to partial hydrolysis of zein under gastric conditions by pepsin, which confers resistance to complete digestion and results in higher bioaccessibility rates. Subsequently, zein is further digested in the intestinal phase by pancreatin proteases, including trypsin, promoting faster release at intestinal level of the bioactive compounds [74].

Flavonoids such as hesperidin and rutin can bind pepsin, hesperidin specifically to its catalytic residue, reducing zein-particle hydrolysis, preserving particle integrity, and protecting encapsulated phenolics [75]. In this study, the recoveries of narirutin and hesperidin exceeded 100%, due to their presence in control microparticles from citrus pectin (Table 5).

In general, phenolic degradation mainly occurs during the intestinal phase, largely due to alkaline pH conditions [5,76]. However, phenolic stability during digestion is strongly compound-dependent. For instance, quercetin glycosides exhibit greater stability than their aglycone forms, while rutinosides such as rutin show significant losses, with approximately 40% degradation following *in vitro* digestion (see Figure 7). Accordingly, flavonols consistently exhibited the lowest bioaccessibility (< 60%), which agrees with the results of the present study and those reported in the literature. On the other hand, flavanone glycosides, including narirutin and hesperidin, demonstrated lower bioaccessibility compared to their corresponding aglycones, naringenin and hesperetin, which is likely attributable to differences in solubility [77,78].

Lime-loaded microparticles incorporated into gluten-free vegan pancakes showed differences in phenolic compounds digestion, influenced by the food matrix. Components like fibre and proteins interacted with the microparticles, affecting phenolic release, solubility, stability, and bioaccessibility.

Narirutin, hesperidin and rutin showed markedly reduced bioaccessibility and recovery in pancakes, especially compared to the particles alone. This reduction is attributed to interactions with the high starch content of rice flour and the increased dietary fibre contributed by the lime-loaded particles (Table 6), which can effectively bind phenolic compounds through hydrogen bonding and Van der Waals forces, thereby limiting their release [79,80]. Additionally, phenolics form insoluble complexes with soybean and chickpea proteins through hydrophobic interactions, whereby the aromatic rings of polyphenols bind to the hydrophobic regions of proteins. These interactions further limit phenolic release, leading to reduced recovery and bioaccessibility [81,82]

In contrast, ferulic acid showed an opposite trend, showing higher levels in pancakes compared with both extract and particles. This increase is linked to the presence of bound ferulic acid in chickpea flour and pectin, which can be released during digestion [83,84]. Its absence in the control pancake is probably due to the low chickpea flour content, and the lack of ferulic acid dehydrodimers in rice flour [85]. Moreover, the pancake preparation process may have facilitated partial hydration and solubilization of the particles, promoting ferulic acid release through mixing and brief baking-powder-induced fermentation. These processing effects likely enhanced ferulic acid availability, resulting in higher levels detected after *in vitro* digestion [86].

This study demonstrates that zein–pectin microparticles are an effective delivery system for protecting phenolic compounds from lime by-products under gastrointestinal conditions. Furthermore, these microparticles proved suitable for incorporation into a baked food matrix, such as pancakes. In this context, they effectively preserved phenolic stability, modulated release during digestion, and enabled functional food enrichment without compromising bioaccessibility. These findings highlight the critical role of both encapsulation and food matrix interactions in determining phenolic fate during digestion.

Further research should explore different food matrices to elucidate how key physicochemical attributes—moisture, protein composition, and dietary fibre content—influence microparticle integrity, and phenolic release, thus supporting the rational design of optimised phenolic-enriched foods.

ARTICLE

7.1. *In vitro* digestion of free extract and lime-loaded microparticles.

7.1.1

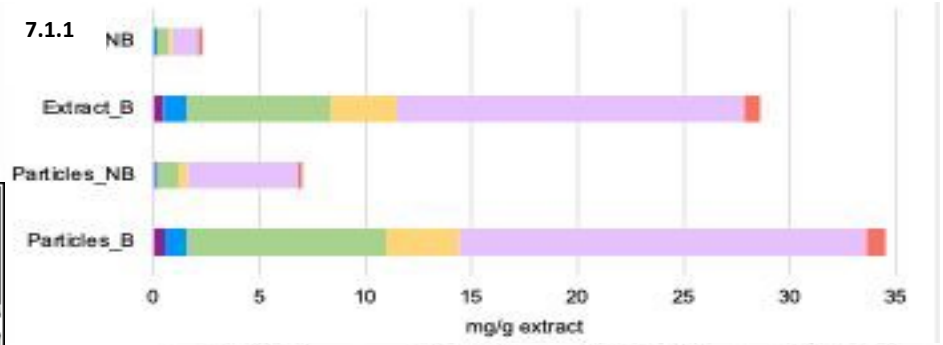

7.1.2.

	Extract_%B	Extract_%R	Particles_%B	Particles_%R
Chlorogenic acid	113	128	119	137
Ferulic acid	59	63	58	66
Eriocitrin	45	48	63	69
Narirutin	81	85	93	104
Hesperidin	85	90	95	120
Rutin	44	55	59	72

Σ	B fraction (mg/g extract)	NB fraction (mg/g extract)	TOTAL (mg/g extract)	% B	% R
Extract	28.60	2.30	30.90	71.45 ± 26.88	78.07 ± 29.55
Particles	34.46	7.05	41.51	81.14 ± 24.88	95.02 ± 30.10

7.2 *In vitro* digestion of enriched pancakes with lime-loaded microparticles.

7.2.1

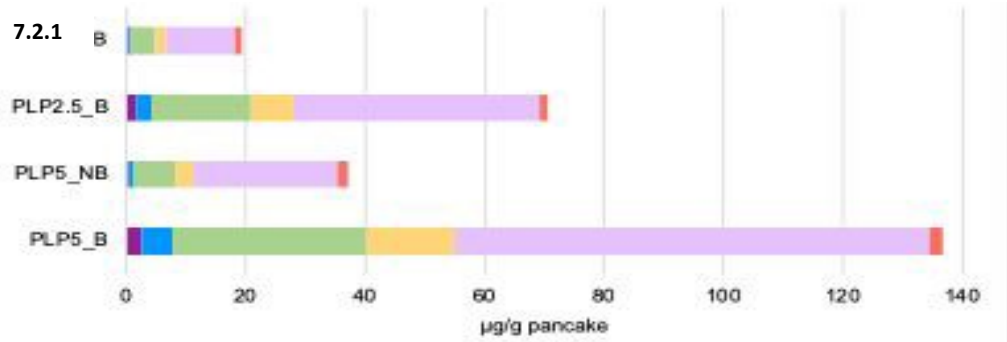

7.2.2.

	PLP2.5_%B	PLP2.5_%R	PLP5_%B	PLP5_%R
Chlorogenic acid	57	67	64	73
Ferulic acid	76	89	76	91
Eriocitrin	69	86	63	77
Narirutin	59	73	65	78
Hesperidin	56	72	54	70
Rutin	27	47	25	42

Σ	B fraction (µg/g pancake)	NB fraction (µg/g pancake)	TOTAL (µg/g pancake)	% B	% R
PLP2.5	70.32	19.21	89.53	57.39± 16.60	72.35 ± 15.21
PLP5	136.75	37.01	173.76	57.79 ± 17.71	71.90 ± 16.05

Figure 7. Results obtained after *in vitro* digestion: 7.1.1.) total amounts in the bioaccessible and non-bioaccessible fractions of each phenolic compound quantified in the extract and lime-loaded microparticles; 7.2.1.) total amounts in the bioaccessible and non-bioaccessible fractions of each phenolic compound quantified in enriched pancake; 7.1.2.) bioaccessibility and recovery percentages of each phenolic compound after *in vitro* digestion of unencapsulated extract and lime-loaded microparticles; 7.2.2.) bioaccessibility and recovery percentages of each phenolic compound after *in vitro* digestion of enriched pancakes. The table below shows the overall bioaccessible and non bioaccessible fraction, as well as the average percentages of bioaccessibility and recovery. #PC was not included in the graph due absence of quantifiable phenolic compounds in any fractions.
B: bioaccessible fraction; NB: not bioaccessible fraction; %B: percentage of bioaccessibility considering the initial content; %R: recovery percentage fraction considering the initial content. PC: pancake control did not display any phenolic compound. PLP2.5: pancake fortified at 2.5%; PLP5: pancake fortified at 5%.

View Article Online
DOI: 10.1039/D6FB00090H

ARTICLE

4. Conclusions

This study demonstrates the successful valorisation of lime by-products into functional ingredients using nano- and mini- spray drying.

It is important to highlight that the study adopts an application-oriented perspective, evaluating the performance of these encapsulated systems under laboratory and pilot-scale processing conditions. This approach provides practical information on the formulation's feasibility and potential considerations for its possible industrial production.

Zein–pectin microparticles effectively protected phenolic compounds under thermal and digestive conditions, preserving the phenolic composition and providing high bioaccessibility. Their incorporation into gluten-free, vegan pancakes improved both the nutritional and functional profiles, addressing current challenges associated with the nutritional quality of some gluten-free and vegan bakery products.

Further studies are needed to evaluate the performance and stability of these functional particles across a wider range of food applications, in order to better understand their effectiveness and adaptability within different food matrices. Moreover, future work should include a sensory evaluation to fully assess consumer acceptance and product viability.

Overall, these findings underscore the potential of combining innovative encapsulation techniques with circular economy principles to develop sustainable, health-promoting food products.

Author contributions. CRediT

Conceptualization, S.M.-C., R.T., L.B.-P.; methodology, S.M.-C., R.T., L.B.-P. ; validation, R.T., F.F., A.R.B.Q., R.S., L.B.-P.; formal analysis, S.M.-C.; investigation, S.M.-C.; resources, L.B.-P. and F.F; data curation, S.M.-C.; writing—original draft preparation, S.M.-C.; writing— review and editing, S.M.-C., R.T., A.R.B.Q., R.S., L.B.-P.; supervision, R.T. and L.B.-P..; project administration, L.B.-P.; funding acquisition, L.B.-P.

Conflicts of interest

There are no conflicts to declare.

Data availability

The data supporting the findings of this study are available from the corresponding a uthor upon reasonable request. All relevant data generated or analyzed during this study are included within the article and its supplementary materials. Further details regarding experimental procedures, raw data, and analytical methods can be provided to qualified researchers to ensure transparency and reproducibility of the results.

Acknowledgements

Sandra Mariño-Cortegoso is grateful to her fellowship within the framework of the ERASMUS+ Program, 2023-1-ES01-KA131-HED-000135235. Authors would like to thank the use of RIAIDT-USC analytical facilities. We also thank Carlos A. García González and José Víctor Álvarez from the Department of Pharmaceutical Technology for generously providing access to their equipment, as well as for their valuable support and time.

References

1. Caldeira C, De Laurentiis V, Corrado S, van Holsteijn F, Sala S. Quantification of food waste per product group along the food supply chain in the European Union: a mass flow analysis. Resour Conserv Recycl. 2019 Oct;149:479–88. doi:10.1016/j.resconrec.2019.06.011
2. Ortiz-Sanchez M, Cardona Alzate CA, Solarte-Toro JC. Orange Peel Waste as a Source of Bioactive Compounds and Valuable Products: Insights Based on Chemical Composition and Biorefining. Biomass. 2024 Feb 2;4(1):107–31. doi:10.3390/biomass4010006
3. Sánchez-Bravo P, Costa-Pérez A, García-Viguera C, Domínguez-Perles R, Medina S. Prevention of inflammation and oxidative stress by new ingredients based on high (poly)phenols winery by-products. JSFA reports. 2025 Feb 12;5(2):40–9. doi:10.1002/jsf2.224
4. Torres-Fuentes C, Suárez M, Aragonès G, Mulero M, Ávila-Román J, Arola-Arnal A, et al. Cardioprotective Properties of Phenolic Compounds: A Role for Biological Rhythms. Mol Nutr Food Res. 2022 Nov 28;66(21). doi:10.1002/mnfr.202100990
5. Gómez-Mejía E, Sacristán I, Rosales-Conrado N, León-González ME, Madrid Y. Valorization of Citrus reticulata Blanco Peels to Produce Enriched Wheat Bread: Phenolic Bioaccessibility and Antioxidant Potential. Antioxidants. 2023 Sep 8;12(9):1742. doi:10.3390/antiox12091742
6. Ribas-Agustí A, Martín-Belloso O, Soliva-Fortuny R, Elez-Martínez P. Food processing strategies to enhance phenolic compounds bioaccessibility and bioavailability in plant-

based foods. Crit Rev Food Sci Nutr. 2018 Oct 13;58(15):2531–48. doi:10.1080/10408398.2017.1331200

7. Zhang H, Wang M, Xiao J. Stability of polyphenols in food processing. In: Toldrá F, editor. Advances in Food and Nutrition Research, volume 102. Advances in Food and Nutrition Research; 2022. p. 1–45. doi:10.1016/bs.afnr.2022.04.006
8. Bińkowska W, Szpicer A, Stelmasiak A, Wojtasik-Kalinowska I, Półtorak A. Microencapsulation of Polyphenols and Their Application in Food Technology. Applied Sciences. 2024 Dec 20;14(24):11954. doi:10.3390/app142411954
9. Zhou H, Zheng B, McClements DJ. *In Vitro* Gastrointestinal Stability of Lipophilic Polyphenols is Dependent on their Oil–Water Partitioning in Emulsions: Studies on Curcumin, Resveratrol, and Quercetin. J Agric Food Chem. 2021 Mar 24;69(11):3340–50. doi:10.1021/acs.jafc.0c07578
10. Chang C, Wang T, Hu Q, Luo Y. Zein/caseinate/pectin complex nanoparticles: Formation and characterization. Int J Biol Macromol. 2017 Nov;104:117–24. doi:10.1016/j.ijbiomac.2017.05.178
11. Sun N, Chen C, Zhu F. Encapsulation of ferulic acid in quinoa protein and zein nanoparticles prepared through antisolvent precipitation: Structure, stability and gastrointestinal digestion. Food Biosci. 2025 Jun;68:106760. doi:10.1016/j.fbio.2025.106760
12. Zhang Z, Meng Y, Wang J, Qiu C, Miao W, Lin Q, et al. Preparation and characterization of zein-based core-shell nanoparticles for encapsulation and delivery of hydrophobic nutrient molecules: Enhancing environmental stress resistance and antioxidant activity. Food Hydrocoll. 2024 Mar;148:109524. doi:10.1016/j.foodhyd.2023.109524
13. Elmizadeh A, Goli SAH, Mohammadifar MA, Rahimmalek M. Fabrication and characterization of pectin-zein nanoparticles containing tanshinone using anti-solvent precipitation method. Int J Biol Macromol. 2024 Mar;260:129463. doi:10.1016/j.ijbiomac.2024.129463
14. Majzoobi M, Vosooghi Poor Z, Mesbahi G, Jamalian J, Farahnaky A. Effects of carrot pomace powder and a mixture of pectin and xanthan on the quality of gluten-free batter and cakes. J Texture Stud. 2017 Dec 5;48(6):616–23. doi:10.1111/jtxs.12276
15. Sharma P, Osama K, Gaur VK, Farooqui A, Varjani S, Younis K. Sustainable utilization of Citrus limetta peel for obtaining pectin and its application in cookies as a fat replacer. J Food Sci Technol. 2023 Mar 13;60(3):975–86. doi:10.1007/s13197-022-05424-1
16. Díaz-Montes E. Wall Materials for Encapsulating Bioactive Compounds via Spray-Drying: A Review. Polymers (Basel). 2023 Jun 12;15(12):2659. doi:10.3390/polym15122659
17. Kandasamy S, Naveen R. A review on the encapsulation of bioactive components using spray-drying and freeze-drying techniques. J Food Process Eng. 2022 Aug 22;45(8). doi:10.1111/jfpe.14059
18. De La Cruz-Molina A V., Gonçalves C, Neto MD, Pastrana L, Jauregi P, Amado IR. Whey–pectin microcapsules improve the stability of grape marc phenolics during digestion. J Food Sci. 2023 Dec 31;88(12):4892–906. doi:10.1111/1750-3841.16806
19. Xue J, Wang T, Hu Q, Zhou M, Luo Y. Insight into natural biopolymer-emulsified solid lipid nanoparticles for encapsulation of curcumin: Effect of loading methods. Food Hydrocoll. 2018 Jun;79:110–6. doi:10.1016/j.foodhyd.2017.12.018
20. Di Cairano M, Galgano F, Tolve R, Caruso MC, Condelli N. Focus on gluten free biscuits: Ingredients and issues. Trends Food Sci Technol. 2018 Nov;81:203–12. doi:10.1016/j.tifs.2018.09.006
21. Di Nardo G, Villa MP, Conti L, Ranucci G, Pacchiarotti C, Principessa L, et al. Nutritional deficiencies in children with celiac disease resulting from a gluten-free diet: a systematic review. Nutrients. 2019 Jul 1;11(7). doi:10.3390/nu11071588 PubMed PMID: 31337023.
22. Temple NJ. A rational definition for functional foods: A perspective. Front Nutr. 2022 Sep 29;9. doi:10.3389/fnut.2022.957516
23. Mateus ARS, Mariño-Cortegoso S, Barros SC, Sendón R, Barbosa L, Pena A, et al. Citrus by-products: A dual assessment of antioxidant properties and food contaminants towards circular economy. Innovative Food Science and Emerging Technologies. 2024 Jul 1;95. doi:10.1016/j.ifset.2024.103737
24. Brodkorb A, Egger L, Alminger M, Alvito P, Assunção R, Ballance S, et al. INFOGEST static in vitro simulation of gastrointestinal food digestion. Nat Protoc. 2019 Apr 18;14(4):991–1014. doi:10.1038/s41596-018-0119-1
25. Rodsamran P, Sothornvit R. Extraction of phenolic compounds from lime peel waste using ultrasonic-assisted and microwave-assisted extractions. Food Biosci. 2019 Apr;28:66–73. doi:10.1016/j.fbio.2019.01.017
26. Silva PM, Prieto C, Andrade CCP, Lagarón JM, Pastrana LM, Coimbra MA, et al. Hydroxypropyl methylcellulose-based micro- and nanostructures for encapsulation of melanoidins: Effect of electrohydrodynamic processing variables on morphological and physicochemical properties. Int J Biol Macromol. 2022 Mar;202:453–67. doi:10.1016/j.ijbiomac.2022.01.019
27. Duhoranimana E, Yu J, Mukeshimana O, Habinshuti I, Karangwa E, Xu X, et al. Thermodynamic characterization of Gelatin–Sodium carboxymethyl cellulose complex coacervation encapsulating Conjugated Linoleic Acid (CLA). Food Hydrocoll. 2018 Jul;80:149–59. doi:10.1016/j.foodhyd.2018.02.011
28. Wang B, Adhikari B, Barrow CJ. Optimisation of the microencapsulation of tuna oil in gelatin–sodium hexametaphosphate using complex coacervation. Food Chem. 2014 Sep;158:358–65. doi:10.1016/j.foodchem.2014.02.135
29. European Parliament C of the EU. Regulation (EU) No 1169/2011 of the European Parliament and of the Council of 25 October 2011 on the provision of food information to consumers [Internet]. 304. 2011 Oct 25. p. 18–63. Available from: https://eur-lex.europa.eu/legal-content/EN/TXT/?uri=CELEX:32011R1169
30. Asociación Española de Normalización (UNE). UNE-EN ISO/IEC 17025:2017. General requirements for the competence of testing and calibration laboratories. Spain; 2017 Dec 20.
31. Bianchi F, Cervini M, Giuberti G, Rocchetti G, Lucini L, Simonato B. Distilled grape pomace as a functional ingredient in vegan muffins: effect on physicochemical, nutritional, rheological and sensory aspects. Int J Food Sci Technol. 2022 Aug 4;57(8):4847–58. doi:10.1111/ijfs.15720

32. Bruttomesso M, Bianchi F, Pasqualoni I, Rizzi C, Simonato B. Evaluation of the technological and compositional features of pancakes fortified with Acheta domesticus. LWT. 2024 May;199:116073. doi:10.1016/j.lwt.2024.116073
33. Singleton VL, Rossi JA. Colorimetry of Total Phenolics with Phosphomolybdic-Phosphotungstic Acid Reagents. Am J Enol Vitic. 1965;16(3):144–58. doi:10.5344/ajev.1965.16.3.144
34. Herald TJ, Gadgil P, Tilley M. High-throughput micro plate assays for screening flavonoid content and DPPH-scavenging activity in sorghum bran and flour. J Sci Food Agric. 2012 Aug 30;92(11):2326–31. doi:10.1002/jsfa.5633
35. Herald TJ, Gadgil P, Perumal R, Bean SR, Wilson JD. High-throughput micro-plate <scp>HCl</scp> –vanillin assay for screening tannin content in sorghum grain. J Sci Food Agric. 2014 Aug 24;94(10):2133–6. doi:10.1002/jsfa.6538
36. Barbosa-Pereira L, Guglielmetti A, Zeppa G. Pulsed Electric Field Assisted Extraction of Bioactive Compounds from Cocoa Bean Shell and Coffee Silverskin. Food Bioproc Tech. 2018 Apr 1;11(4):818–35. doi:10.1007/s11947-017-2045-6
37. von Gadow A, Joubert E, Hansmann CF. Comparison of the Antioxidant Activity of Aspalathin with That of Other Plant Phenols of Rooibos Tea (*Aspalathus linearis*), α-Tocopherol, BHT, and BHA. J Agric Food Chem. 1997 Mar 1;45(3):632–8. doi:10.1021/jf960281n
38. Andrade MA, de Oliveira Torres LR, Silva AS, Barbosa CH, Vilarinho F, Ramos F, et al. Industrial multi-fruits juices by-products: total antioxidant capacity and phenolics profile by LC–MS/MS to ascertain their reuse potential. European Food Research and Technology. 2020 Nov 27;246(11):2271–82. doi:10.1007/s00217-020-03571-3
39. Shukla R, Cheryan M. Zein: the industrial protein from corn. Ind Crops Prod. 2001 May;13(3):171–92. doi:10.1016/S0926-6690(00)00064-9
40. Yang J, Lin J, Zhang J, Chen X, Wang Y, Shen M, et al. Fabrication of Zein/ *Mesona chinensis* Polysaccharide Nanoparticles: Physical Characteristics and Delivery of Quercetin. ACS Appl Bio Mater. 2022 Apr 18;5(4):1817–28. doi:10.1021/acsabm.2c00209
41. Guo Q, Su J, Shu X, Yuan F, Mao L, Liu J, et al. Production and characterization of pea protein isolate-pectin complexes for delivery of curcumin: Effect of esterified degree of pectin. Food Hydrocoll. 2020 Aug;105:105777. doi:10.1016/j.foodhyd.2020.105777
42. Huang X, Liu Y, Zou Y, Liang X, Peng Y, McClements DJ, et al. Encapsulation of resveratrol in zein/pectin core-shell nanoparticles: Stability, bioaccessibility, and antioxidant capacity after simulated gastrointestinal digestion. Food Hydrocoll. 2019 Aug;93:261–9. doi:10.1016/j.foodhyd.2019.02.039
43. Sharma SK, Gupta SM. Preparation and evaluation of stable nanofluids for heat transfer application: A review. Exp Therm Fluid Sci. 2016 Dec;79:202–12. doi:10.1016/j.expthermflusci.2016.06.029
44. De Cicco F, Porta A, Sansone F, Aquino RP, Del Gaudio P. Nanospray technology for an in situ gelling nanoparticulate powder as a wound dressing. Int J Pharm. 2014;473(1):30–7. doi:https://doi.org/10.1016/j.ijpharm.2014.06.049
45. Silva PM, Prieto C, Lagarón JM, Pastrana LM, Coimbra MA, Vicente AA, et al. Food-grade hydroxypropyl methylcellulose-based formulations for electrohydrodynamic processing: Part I. Role of solution parameters on fibre and particle production. Food Hydrocoll. 2021 Sep;118:106761. doi:10.1016/j.foodhyd.2021.106761
46. Li X, Anton N, Arpagaus C, Belleteix F, Vandamme TF. Nanoparticles by spray drying using innovative new technology: The Büchi Nano Spray Dryer B-90. Journal of Controlled Release. 2010 Oct;147(2):304–10. doi:10.1016/j.jconrel.2010.07.113
47. Bichara LC, Alvarez PE, Fiori Bimbi M V., Vaca H, Gervasi C, Brandán SA. Structural and spectroscopic study of a pectin isolated from citrus peel by using FTIR and FT-Raman spectra and DFT calculations. Infrared Phys Technol. 2016 May;76:315–27. doi:10.1016/j.infrared.2016.03.009
48. La Cava EL, Gerbino E, Sgroppo SC, Gómez-Zavaglia A. Characterization of Pectins Extracted from Different Varieties of Pink/Red and White Grapefruits [*Citrus Paradisi* (Macf.)] by Thermal Treatment and Thermosonication. J Food Sci. 2018 Jun 22;83(6):1613–21. doi:10.1111/1750-3841.14183
49. Lei Y, Wu H, Jiao C, Jiang Y, Liu R, Xiao D, et al. Investigation of the structural and physical properties, antioxidant and antimicrobial activity of pectin-konjac glucomannan composite edible films incorporated with tea polyphenol. Food Hydrocoll. 2019 Sep;94:128–35. doi:10.1016/j.foodhyd.2019.03.011
50. Wang W, Ma X, Jiang P, Hu L, Zhi Z, Chen J, et al. Characterization of pectin from grapefruit peel: A comparison of ultrasound-assisted and conventional heating extractions. Food Hydrocoll. 2016 Dec;61:730–9. doi:10.1016/j.foodhyd.2016.06.019
51. López de Dicastillo C, Piña C, Garrido L, Arancibia C, Galotto MJ. Enhancing Thermal Stability and Bioaccesibility of Açaí Fruit Polyphenols through Electrohydrodynamic Encapsulation into Zein Electrosprayed Particles. Antioxidants. 2019 Oct 9;8(10):464. doi:10.3390/antiox8100464
52. Chen TT, Zhang ZH, Wang ZW, Chen ZL, Ma H, Yan JK. Effects of ultrasound modification at different frequency modes on physicochemical, structural, functional, and biological properties of citrus pectin. Food Hydrocoll. 2021 Apr;113:106484. doi:10.1016/j.foodhyd.2020.106484
53. Hu K, Huang X, Gao Y, Huang X, Xiao H, McClements DJ. Core–shell biopolymer nanoparticle delivery systems: Synthesis and characterization of curcumin fortified zein–pectin nanoparticles. Food Chem. 2015 Sep;182:275–81. doi:10.1016/j.foodchem.2015.03.009
54. Huang X, Dai Y, Cai J, Zhong N, Xiao H, McClements DJ, et al. Resveratrol encapsulation in core-shell biopolymer nanoparticles: Impact on antioxidant and anticancer activities. Food Hydrocoll. 2017 Mar;64:157–65. doi:10.1016/j.foodhyd.2016.10.029
55. RamachandraRao Sonale S, Pothuvan Kunnummal S, Sori N, Reddy JP, Khan M. Low methoxy feruloylated pectin from beetroot: Antioxidant and prebiotic properties. J Food Process Preserv. 2022 Dec 26;46(12). doi:10.1111/jfpp.17240
56. Esparza-Martínez FJ, Miranda-López R, Guzman-Maldonado SH. Effect of air-drying temperature on extractable and non-extractable phenolics and antioxidant capacity of lime

wastes. Ind Crops Prod. 2016 Jun;84:1–6. doi:10.1016/j.indcrop.2016.01.043

57. European Parliament C of the EU. Regulation (EC) No 1924/2006 of the European Parliament and of the Council of 20 December 2006 on nutrition and health claims made on foods [Internet]. 404. 2006 Dec 20. p. 9–25. Available from: https://eur-lex.europa.eu/eli/reg/2006/1924/oj
58. Cirrincione F, Ferranti P, Ferrara A, Romano A. A critical evaluation on the valorization strategies to reduce and reuse orange waste in bakery industry. Food Research International. 2024 Jul;187:114422. doi:10.1016/j.foodres.2024.114422
59. Zahorec J, Šoronja-Simović D, Petrović J, Nikolić I, Pavlić B, Bijelić K, et al. Fortification of Bread with Carob Extract: A Comprehensive Study on Dough Behavior and Product Quality. Foods. 2025 May 20;14(10):1821. doi:10.3390/foods14101821
60. Kabisch S, Honsek C, Kemper M, Gerbracht C, Arafat AM, Birkenfeld AL, et al. Dose-dependent effects of insoluble fibre on glucose metabolism: a stratified post hoc analysis of the Optimal Fibre Trial (OptiFiT). Acta Diabetol. 2021 Dec 12;58(12):1649–58. doi:10.1007/s00592-021-01772-0
61. Weickert MO, Pfeiffer AF. Impact of Dietary Fiber Consumption on Insulin Resistance and the Prevention of Type 2 Diabetes. J Nutr. 2018 Jan;148(1):7–12. doi:10.1093/jn/nxx008
62. Leroux J, Langendorff V, Schick G, Vaishnav V, Mazoyer J. Emulsion stabilizing properties of pectin. Food Hydrocoll. 2003 Jul;17(4):455–62. doi:10.1016/S0268-005X(03)00027-4
63. Mileti O, Baldino N, Luzzi S, Lupi FR, Gabriele D. Interfacial Rheological Study of β-Casein/Pectin Mixtures at the Air/Water Interface. Gels. 2024 Jan 3;10(1):41. doi:10.3390/gels10010041
64. Elgeti D, Jekle M, Becker T. Strategies for the aeration of gluten-free bread – A review. Trends Food Sci Technol. 2015 Nov;46(1):75–84. doi:10.1016/j.tifs.2015.07.010
65. Djordjević M, Djordjević M, Šoronja-Simović D, Nikolić I, Šereš Z. Delving into the Role of Dietary Fiber in Gluten-Free Bread Formulations: Integrating Fundamental Rheological, Technological, Sensory, and Nutritional Aspects. Polysaccharides. 2021 Dec 30;3(1):59–82. doi:10.3390/polysaccharides3010003
66. Cuomo F, Iacovino S, Cinelli G, Messia MC, Marconi E, Lopez F. Effect of additives on chia mucilage suspensions: A rheological approach. Food Hydrocoll. 2020 Dec;109:106118. doi:10.1016/j.foodhyd.2020.106118
67. Akshata B, Indrani D, Prabhasankar P. Effects of ingredients and certain additives on rheological and sensory characteristics of gluten-free eggless pancake. J Food Process Preserv. 2019 Oct 28;43(10). doi:10.1111/jfpp.14129
68. Jantathai S, Sungsri-in M, Mukprasirt A, Duerrschmid K. Sensory expectations and perceptions of Austrian and Thai consumers: A case study with six colored Thai desserts. Food Research International. 2014 Oct;64:65–73. doi:10.1016/j.foodres.2014.06.007
69. Öncel B. Investigation of physicochemical, bioactive, textural and sensory properties of gluten-free cakes enriched with kumquat (little jewel of citrus) flour. Journal of Food Measurement and Characterization. 2025 Aug 27;19(8):5787–95. doi:10.1007/s11694-025-03354-y
70. Kırbaş Z, Kumcuoglu S, Tavman S. Effects of apple, orange and carrot pomace powders on gluten-free batter rheology and cake properties. J Food Sci Technol. 2019 Feb 11;56(2):914–26. doi:10.1007/s13197-018-03554-z
71. Maghsoud M, Heshmati A, Taheri M, Emamifar A, Esfarjani F. The influence of carboxymethyl cellulose and hydroxypropyl methylcellulose on physicochemical, texture, and sensory characteristics of gluten-free pancake. Food Sci Nutr. 2024 Feb 20;12(2):1304–17. doi:10.1002/fsn3.3844
72. Hu Y, Zhang W, Ke Z, Li Y, Zhou Z. In vitro release and antioxidant activity of Satsuma mandarin (*Citrus reticulata* Blanco cv. unshiu) peel flavonoids encapsulated by pectin nanoparticles. Int J Food Sci Technol. 2017 Nov 10;52(11):2362–73. doi:10.1111/ijfs.13520
73. Liang X, Cao K, Li W, Li X, McClements DJ, Hu K. Tannic acid-fortified zein-pectin nanoparticles: Stability, properties, antioxidant activity, and in vitro digestion. Food Research International. 2021 Jul;145:110425. doi:10.1016/j.foodres.2021.110425
74. Zou L, Zheng B, Zhang R, Zhang Z, Liu W, Liu C, et al. Enhancing the bioaccessibility of hydrophobic bioactive agents using mixed colloidal dispersions: Curcumin-loaded zein nanoparticles plus digestible lipid nanoparticles. Food Research International. 2016 Mar;81:74–82. doi:10.1016/j.foodres.2015.12.035
75. Yu J, Li X, Liu H, Peng Y, Wang X, Xu Y. Interaction behavior between five flavonoids and pepsin: Spectroscopic analysis and molecular docking. J Mol Struct. 2021 Jan;1223:128978. doi:10.1016/j.molstruc.2020.128978
76. Tenore GC, Campiglia P, Giannetti D, Novellino E. Simulated gastrointestinal digestion, intestinal permeation and plasma protein interaction of white, green, and black tea polyphenols. Food Chem. 2015 Feb;169:320–6. doi:10.1016/j.foodchem.2014.08.006
77. Pinacho R, Cavero RY, Astiasarán I, Ansorena D, Calvo MI. Phenolic compounds of blackthorn (Prunus spinosa L.) and influence of in vitro digestion on their antioxidant capacity. J Funct Foods. 2015 Dec;19:49–62. doi:10.1016/j.jff.2015.09.015
78. Li CX, Wang FR, Zhang B, Deng ZY, Li HY. Stability and antioxidant activity of phenolic compounds during in vitro digestion. J Food Sci. 2023 Feb 8;88(2):696–716. doi:10.1111/1750-3841.16440
79. Bordenave N, Hamaker BR, Ferruzzi MG. Nature and consequences of non-covalent interactions between flavonoids and macronutrients in foods. Food Funct. 2014;5(1):18–34. doi:10.1039/C3FO60263J
80. Shahidi F, Pan Y. Influence of food matrix and food processing on the chemical interaction and bioaccessibility of dietary phytochemicals: A review. Crit Rev Food Sci Nutr. 2022 Aug 11;62(23):6421–45. doi:10.1080/10408398.2021.1901650
81. Jia Y, Fu Y, Man H, Yan X, Huang Y, Sun S, et al. Comparative study of binding interactions between different dietary flavonoids and soybean β-conglycinin and glycinin: Impact on structure and function of the proteins. Food Research International. 2022 Nov;161:111784. doi:10.1016/j.foodres.2022.111784
82. Jia Y, Yan X, Huang Y, Zhu H, Qi B, Li Y. Different interactions driving the binding of soy proteins (7S/11S) and flavonoids (quercetin/rutin): Alterations in the conformational and

View Article Online
DOI: 10.1039/D6FB00090H

functional properties of soy proteins. Food Chem. 2022 Dec;396:133685. doi:10.1016/j.foodchem.2022.133685

83. Sreerama YN, Sashikala VB, Pratape VM. Variability in the Distribution of Phenolic Compounds in Milled Fractions of Chickpea and Horse Gram: Evaluation of Their Antioxidant Properties. J Agric Food Chem. 2010 Jul 28;58(14):8322–30. doi:10.1021/jf101335r

84. Wang C, Cai W, Yao J, Wu L, Li L, Zhu J, et al. Conjugation of ferulic acid onto pectin affected the physicochemical, functional and antioxidant properties. J Sci Food Agric. 2020 Dec 14;100(15):5352–62. doi:10.1002/jsfa.10583

85. Bunzel M, Ralph J, Marita JM, Hatfield RD, Steinhart H. Diferulates as structural components in soluble and insoluble cereal dietary fibre. J Sci Food Agric. 2001 May 15;81(7):653–60. doi:10.1002/jsfa.861

86. Đorđević TM, Šiler-Marinković SS, Dimitrijević-Branković SI. Effect of fermentation on antioxidant properties of some cereals and pseudo cereals. Food Chem. 2010 Apr 1;119(3):957–63. doi:10.1016/j.foodchem.2009.07.049

View Article Online
DOI: 10.1039/D6FB00090H

USC UNIVERSIDADE DE SANTIAGO DE COMPOSTELA

FoodChemPack
RESEARCH, DEVELOPMENT AND CHEMICAL SAFETY ASSESSMENT ON FOOD AND FOOD CONTACT MATERIALS

Department of Analytical Chemistry, Nutrition and Food Science
FACULTY OF PHARMACY

Letricia Barbosa Pereira, PhD
Associate Professor
letricia.barbosa.pereira@usc.es

Data Availability Statement

The data supporting the findings of this study are available from the corresponding author upon reasonable request. All relevant data generated or analyzed during this study are included within the article and its supplementary materials. Further details regarding experimental procedures, raw data, and analytical methods can be provided to qualified researchers to ensure transparency and reproducibility of the results.

Sincerely,

Letricia Barbosa-Pereira